Characterization of the renal function in Epac1 (RapGef3) knockout mice

Ronja Bjørnstad

This thesis is submitted in partial fulfilment of the requirements for the degree of Master in

Master of Sience

Medical Cell Biology

Department of Biomedicine

Faculty of Medicine and Dentistry

University of Bergen

Spring 2014

Acknowledgements

The work of this thesis was carried out in the Translational Signaling Group at Department of Biomedicine, University of Bergen, from August 2013 to June 2014.

First of all I would like to express my gratitude to my main supervisors Prof. Stein Ove Døskeland and Prof. Olav Tenstad for great guidance and support during these past months. Thank you for answering all my questions, and for all the discussions we have had throughout this time, it has contributed greatly to introduce me to the academic way of thinking.

I want to acknowledge Reidun Kopperud for initiating the project and teaching me the techniques, surgical procedures needed to conduct the animal work. A special thanks to Nina Lied Larsen, for sharing of her experience, and being good company during days in the lab. Moreover I am grateful for the help from Lars Herfindal, Kirsten Marie Brønstad, and Jonathan Soule, for assisting me in experiments that required an extra sett of hands. To the rest of the Translational Signaling Group, thank you for creating a good working environment.

I would like to thank my fellow master students, for making this a memorable year, not only academically, but also socially. Finally I would like to thank friends and family for all the love and support.

Ronja Bjørnstad
Bergen, Spring 2014

Abstract

The discovery of the exchange proteins directly activated by cAMP (Epac) has renewed our knowledge of intracellular cAMP signaling. The Epac1 isoform (RapGef3) shows high expression level in the kidney. *In vitro* studies have suggested multiple roles for Epac in the renal function. The development of an animal model were Epac1 is knocked out ($Epac1^{-/-}$ mice), however, allows for *in vivo* studies on Epac1 possible renal functions. In the present study $Epac1^{-/-}$ mice were compared to their reference wild type (WT) littermates, during baseline conditions as well as after per oral water load with and without presence of the antidiuretic vasopressin analog desmopressin. Under these conditions we measured renal excretion and/or clearance of creatinine, osmolytes, electrolytes, urea, cAMP and albumin. It turned out that $Epac1^{-/-}$ mice showed a normal ability to dilute their urine; Urine osmolality after water load combined with intra-peritoneal saline injection was 232 ± 14.90 in WT and 249 ± 7.377 in $Epac1^{-/-}$ mice. However, the effect of desmopressin on urine osmolality was significantly attenuated in $Epac1^{-/-}$ mice; Urine osmolality after water load and desmopressin was 598 ± 88.37 in WT and 443 ± 33.52 in $Epac1^{-/-}$ animals, with the increase (desmopressin relative to saline) being 163 % in WT and 77 % in $Epac1^{-/-}$ mice. The present study showed that a reduced response to desmopressin could not be explained by under-expression of either the AVP-stimulated urea transporter UT-A1 or the water channel AQP-2. A possibility is that Epac1 is required for optimal trafficking of AQP-2 to the apical membrane. Moreover, creatinine clearance, used as an estimate of glomerular filtration rate, was significantly increased in $Epac1^{-/-}$ mice following water loading (WT; 397 ± 44.98 µl/min vs. $Epac1^{-/-}$ 550 ± 19.52 µl/min). This difference in was not seen after treatment with furosemide (WT; 553 ± 121.9 µl/min vs. $Epac1^{-/-}$ 606 ± 64.01 µl/min), which blocks the Na^+-K^+-$2Cl^-$ co-transporter, and thus the tubulo-glomerular feedback response on vascular tone in the afferent arteriole. Urine and plasma analysis demonstrated no difference in the fractional clearance of osmolytes, creatinine, Na^+, K^+, and urea between WT and $Epac1^{-/-}$ animals. $Epac1^{-/-}$ mice did not demonstrate any sign of proteinuria, suggesting an intact glomerular filtration barrier. We conclude that renal functions are generally well preserved in $Epac1^{-/-}$ mice. These mice do, however, exhibit a moderate polydipsia and polyuria due to a perturbation of the effect of vasopressin on tubular water reabsorption. A role of Epac in the regulation of GFR at the level of *macula densa* is also suggested.

Table of content

Abbreviations

AC	Adenylyl cyclese
AKAP	A-kinase anchoring proteins
AQP-2	Aquaporin-2
ATP	Adenosine triphosphate
AVP	Vasopressin
C	Clearance
cAMP	3´5´cyclic adenosine monophosphate
cAMP-A	Low-affinity cAMP-binding domain
cAMP-B	cAMP-binding domain
CD	Collecting duct
CDC25HD	CDC25-homology domain
cGMP	3´5´ cyclic guanoside monophosphate
CRE	cAMP response element
CREB	cAMP response element binding protein
dDAVP	Desmopressin
DEP	Disheveled-Egl-10-pleckstrin
DT	Distal tubule
EDTA	Ethylenediaminetetraacetic acid
EGTA	Ethylene glycol tetraacetic acid
ENaC	Epithelial sodium channel
Epac	Exchange protein directly activated by cAMP
ERK	Extracellular-signal-regulated kinase
G	Glomerulus
g	Gravitational forces
GDP	Guanosine diphosphate
GFB	Glomerular filtration barrier
GFR	Glomerular filtration rate
GTP	Guanosine triphosphate
Hepes	4-(2-hydroxyethyl)-1-piperazineethanesulfonic acid
HPLC	High pressure liquid chromatography
IMCD	Inner medullary collecting duct
IBMX	3-isobutyl-1-methylxanthine
i.p.	Intra-peritoneal
K_f	Filtration coefficient
LH	Loop of Henle
MD	Macula densa
NHE3	Na^+/H^+ exchanger 3
NKCC2	Na^+-K^+-2Cl co-transporter
NP-40	Nonyl phenoxypolyethoxylethanol-40
PBS	Phosphate buffered saline
PDE	Phosphodiesterase

PKA	Protein kinase A
Pkg1	cGMP-dependent protein kinase 1
Ppia	Peptidylprolyl isomerase A
PT	Proximal tubule
qRT-PCR	Quantitative Reel time-PCR
RA domain	Ras-association domain
REM domain	Ras exchange motif domain
rpm	Revolutions per minute
SDHA	Succinate dehydrogenase complex subunit alpha
SDS	Sodium dodecyl-sulfate
SDS-PAGE	Sodium dodecyl sulfate-polyacrylamide gel electrophoresis
SEM	Standard error of the mean
SGLT	Sodium-glucose co-transporter
TCEP	Tris(2-carboxyethyl)phosphine
TGF	Tubulo-glomerular feedback
UT-A1	Urea transporter A1
UT-A3	Urea transporter A3
UT-B1	Urea transporter B1
WT	Wild type

1 Introduction

1.1 General aspects of Cyclic AMP signaling

The 3´5´cyclic adenosine monophosphate (cAMP) is the archetype of a second messengers, mediating a multitude of important cellular processes (reviewed in (1)). The local concentration and distribution of cAMP is mainly determined by members of the enzyme families adenylyl cyclases (AC's) and cyclic nucleotide phosphodiesterases (PDE's).

Binding of a number of hormones to specific G-protein coupled receptors leads to dissociation and activation of the heterotrimeric G protein, consisting of three subunits, α, β and γ. Multiple classes of α-subunits regulate ACs, and are primarily stimulatory ($G\alpha_s$ family), but can also be inhibitory ($G\alpha_i$ family). The $G\alpha_s$ protein activates AC to catalyze cleavage and cyclisation of ATP to produce cAMP (and PPi). Nine mammalian genes have been identified to encode membrane-bound AC's, whereas only one gene has shown to encode a soluble isoform (reviewed in (2)).

PDE's hydrolyzes cAMP to 5´AMP. There exist 25 mammalian genes encoding PDE's, some with several isoforms and splice variants. They are all divided in 11 PDE families (PDE1–11). PDE4, 7, and 8 selectively recognize cAMP, PDE5, 6, and 9 recognize 3´5´ cyclic guanoside monophosphate (cGMP), while PDE1, 2, 3, 10 and 11 recognize either substrates. PDE's are active enzymes, regulating cAMP signaling. The anchoring of PDE's close to AC is thought to keep the locally produced cAMP confined in local compartments ((3) reviewed in (4)). Another example is through cGMP binding to PDE2 and PDE3. The binding of cGMP to an allosteric site of PDE2 enhances its degradation of cAMP at the active site, while allosteric binding of cGMP inhibits the cAMP degradation by PDE3 ((5, 6) reviewed in (7)).

When intracellular cAMP levels are elevated it can bind to and activate its intracellular receptors (Figure 1). Most central effects of cAMP are mediated by serine/threonine protein kinase A (PKA), ubiquitously expressed in eukaryote cells (8). PKA is a heterotetramer composed of two regulatory (R) and two catalytic (C) subunits. Upon binding of two molecules of cAMP to each R subunit its associated C-subunit dissociates, and becomes free to catalyze phosphorylation of downstream target proteins. It can phosphorylate cytoplasmic polypeptides or translocate into the nucleus to phosphorylate nuclear proteins such as the cAMP response element binding (CREB) protein, which enhances transcription from CRE

element containing promotors. An important action of the R subunit is to anchor PKA to scaffold proteins (AKAP's). The AKAP's serve to confine a proportion of cellular PKA to discrete signaling compartments (reviewed in (9)).

The second family of mammalian cAMP receptors identified is cyclic nucleotide regulated ion channels, first found in photoreceptor cells and olfactory sensory neurons, where they produce membrane depolarization in response to sensory stimuli and cyclic nucleotide binding. They have since been detected also in other cells like cardiomyocytes (reviewed in (10)). The third family identified was the exchange proteins directly activated by cAMP (Epac), described in more detail in section 1.2.

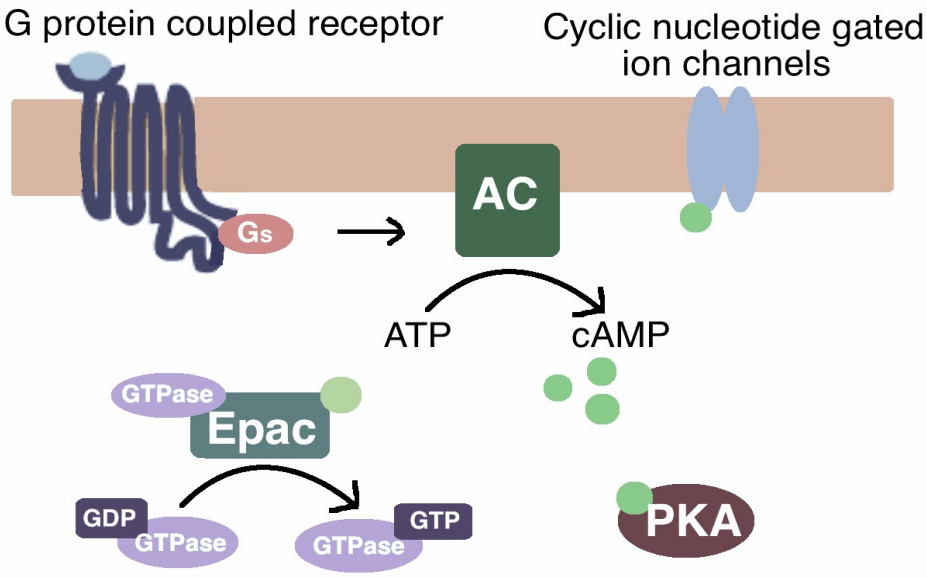

Figure 1: Cyclic AMP signaling pathway. Upon ligand binding to a G-protein coupled receptor, AC will be activated and generate cAMP. An increase in intracellular cAMP acts through three different systems. Most cAMP effects have been attributed to PKA. Binding of cAMP to each R-subunits causes its C subunit to dissociate from the holoenzyme, and is then free to catalyze phosphorylation of downstream proteins. Cyclic nucleotide gated ion channels opens in response to binding of cAMP. Exchange protein directly activated by cAMP (Epac) exchange GDP with GTP on the small GTPases Rap1 and 2. Figure adapted fro Schmidt et al. (11).

1.2 Epac Proteins

Until 1998 the consensus was that cAMP mostly acted via PKA. The finding of the two GDP exchange protein directly activated by cAMP (Epac1, Epac2; RapGef3, 4) opened up a new dimension of cAMP signaling (12, 13). Epac1 was revealed by an *in silico* screen for proteins with cyclic nucleotide binding domains by de Rooji and colleagues (12). Simultaneously, independently of this, Kawasaki et al. discovered Epac2 as a PKA independent activator of

Rap1 (13). Rap1 and Rap2 functions as molecular switches, cycling between an inactive guanosine diphosphate (GDP) bound state and an active guanosine triphosphate (GTP) bound state. Epac promotes the dissociation of bound GDP, and thereby exchanging it with the more abundant GTP (Figure 1). The GTP-bound forms of the Rap proteins can interact specifically with their effector proteins and activate downstream targets (12, 13). The Epac1 and Epac2 proteins exhibit a different expression profile. Epac1 is ubiquitously expressed, albeit with distinct expression level. It is mostly expressed in the kidneys, the hart, blood vessels adipose tissue, ovaries, uterus and the central nervous system. Epac2 splice variants are more tissue specific, mostly abundant in central nervous system, pancreas and adrenal gland (12, 13).

1.2.1 The architecture of Epac

Epac1 and Epac2 are multi domain proteins encoded by two different genes (12), and share extensive sequence homology. As displayed in Figure 2, they both contain an N-terminal regulatory region and a C-terminal catalytic region ((14, 15) reviewed in (11)). The regulatory region contains a high-affinity cAMP-binding domain (cAMP-B) and a membrane-anchoring disheveled-Egl-10-pleckstrin (DEP) domain (14, 16). The DEP-domain is in Epac1 required for its retribution to the plasma membrane (17). Epac2 has an additional low-affinity cAMP-binding domain (cAMP-A) at the N-terminus, found to target one of the Epac2 isoforms to the plasma membrane (14). In the catalytic region the CDC25-homology domain (CDC25HD) with the exchange activity of Epac is located. This in addition to a Ras exchange motif (REM) domain responsible for the GDP-GTP exchange. A Ras-association (RA) domain separates the CDC25HD and the REM domain (14). The N-terminal regulatory region is autoinhibitory and interacts directly with a catalytic region. The theory is that the cAMP binding induces a conformational change that opens the CDC25HD domain from auto inhibitory restrains, and permits GDP-GTP exchange of Rap ((14-16, 18) reviewed in (11)).

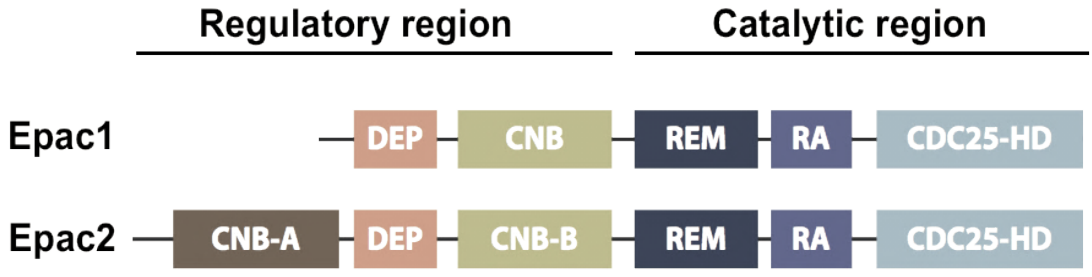

Figure 2: Schematic representation of Epac functional domains. Both Epac 1 and Epac2 contain a N-terminal regulatory region with cAMP-B in Epac 1 and 2 and an additional cAMP-A in Epcac 2. Additionally a DEP domain is located here. The C-terminal catalytic region containing the CDC25-homology domain (CDC25HD) where the exchange activity is located, a REM domain, responsible for the GDP-GTP exchange, and a RA-domain that separates the two. The figure is modified from Gloerich et al. (19).

1.2.2 Methods used to reveal possible biological roles of the Epac proteins

Different tools have been developed to discriminate between PKA and Epac mediated effects of cAMP. Epac and PKA selective cAMP analogs have been developed. Most studies of Epac are based on the use of the Epac activating cAMP analog 8-pCPT-2'-O-methyl-cAMP, which does not activate PKA (20). This analog has however, at high concentrations, several off target effects. One is to inhibit cAMP PDE's and thereby increase cAMP leading to indirect PKA activation (21). Additional off-targets effects are interference with transport proteins (22) and purine receptors (23). Supporting evidence of Epac mediated effects can be obtained if the effect of cAMP cannot be mediated by specific PKA-directed cAMP analogs like N^6-monobutyryl-cAMP or N^6-benzoyl-cAMP (20). Similarly PKA-specific inhibitors can be introduced, to blunt the effect of PKA. A new Epac inhibitor has recently become available, that selectively inhibit the catalytic function of Epac (24). Unfortunately, most studies rely mainly on the one Epac specific cAMP analog 8-pCPT-2'-O-methyl-cAMP. Some of the *in vitro* actions of the Epac analog have been validated by knock down of Epac1 (25, 26). Animal knock out models of the Epac proteins have been developed. The use of these animals is however still in its infancy.

1.2.3 Major (extra-renal) biological roles of Epac

The overall result of cAMP stimulation at the cell or organism level represents the integrated actions of Epac- and PKA-dependent pathways (as well as of cyclic nucleotide regulated ion channels). Several biological roles are implicated for the Epac proteins, either acting alone or synergistically or antagonistically with PKA (reviewed in (27)). An Example of integrated cAMP-PKA-Epac signaling is the formation of a cAMP-responsive signaling complex maintained by AKAP, and includes PKA, a PDE4 and Epac1. These intermolecular interactions facilitate the dissemination of distinct cAMP signals through each effector protein (28). Based mainly on *in vitro* studies, Epac is implicated as cAMP mediator for several renal cell functions including secretion, intracellular Ca^{2+} mobilization, cell adhesion, proliferation, and apoptosis (reviewed in (11)).

In the vasculature there is experimental evidence of Epac having a role in vascular smooth muscle contraction, in addition to being involved in control of the endothelial barrier function. Through signaling via Rap on the actin tubuli network, Epac is thought to enhance cell junction to reduce leakage. Roles of Epac are proposed in the heart, in potentiating

contraction of cardiomyocytes by regulate calcium homeostasis and cardiac hypertrophy (reviewed in (29)). In the lungs Epac may be involved in regulation of airway smooth muscle tone and secretory processes (reviewed in (11)). In pancreas Epac2 is found to be important for regulation of insulin secretion from beta cells. In alpha cells Epac2 mediates induction of glucagon secretion in a PKA-independent manner. Additionally Epac is considered to be a target of cAMP-regulated synaptic potentiation (30).

There are several lines of evidence, both on intact animals and organ and cell culture, that Epac is involved in regulation of neuronal signaling. A role in neuronal differentiation (20) and regeneration has been suggested (reviewed in (31)). Furthermore brain specific Epac1/2 double knock out mice has shown to have learning and memory retrieval and tendencies to autism (32). Epac1 knockout ($Epac1^{-/-}$) mice have altered trans-endothelial uptake of a parasite (33) and possibly altered lipid metabolism (34), although members of our group find no such phenotype in our $Epac1^{-/-}$ mice (S. Døskeland personal communication). The postulated role of Epac in the kidney will be described in section 1.4, after a general introduction to kidney function (1.3).

1.3 Kidney anatomy and function

The kidneys are intricate and highly specialized organs, vital in maintenance of body homeostasis, blood pressure control and in removal of waste products from the body. They are bean shaped organs, lying behind the peritoneum, on each side of the vertebrae. When bisecting a kidney two distinct regions appear, the outer region called the cortex, and the inner region called the medulla (Figure 3A). The functional unit of the kidney is the nephron, and consists of two major components, the renal corpsule and the renal tubules together with the collecting duct (Figure 3B).

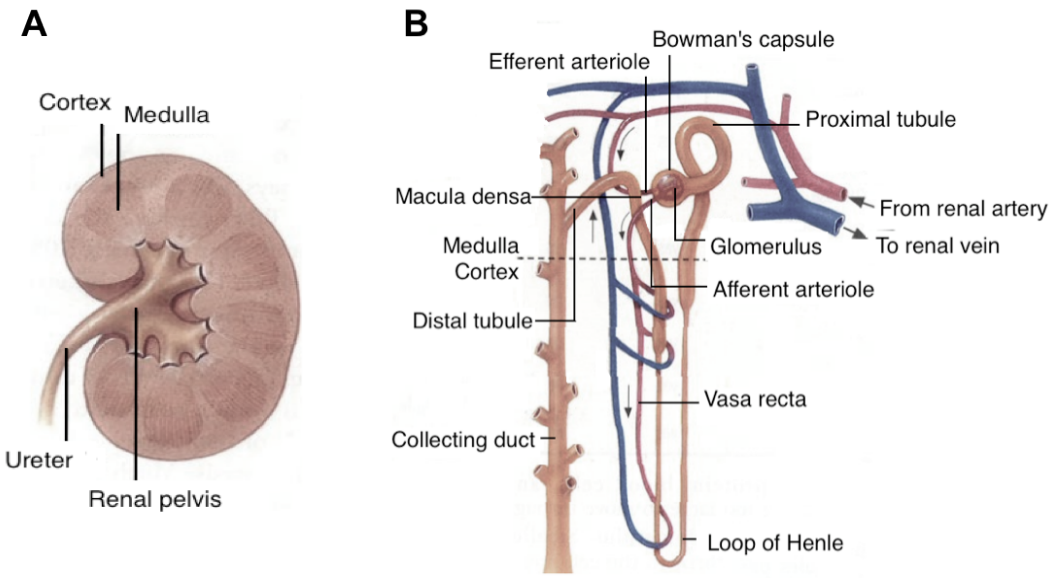

Figure 3: The kidney and its functional unit, the nephron. (A) A bisected kidney revealing two distinct regions, cortex and medulla. Urine is collected in renal pelvis, and further transported to the urine bladder through the ureter. **(B)** In the nephron, plasma is filtered from the glomerulus into Bowman's capsule at a rate of about 125 ml/min in humans (glomerular filtration rate, GFR). The filtrate then continuous into the proximal tubule, were 70% of the fluid is reabsorbed. From there the filter enters the loop of Henle, surrounded by the vasa recta. *Macula densa* is responsible for the tubulo-glomerular feedback control of vascular tone in the afferent arterioles prerequisite for auto regulation of GFR. The filtrate next enters the distal tubule. Several distal tubules join together to form the collecting duct were regulation of water excretion and fine-tuning of salt excretion takes place. Figure adapted from (35).

1.3.1 The renal corpsule

The renal corpsule is located in cortex, and consist of the glomerulus, a tuft of glomerular capillaries, enveloped by the glomerular filtration barrier (GFB), that forms Bowman's capsule. The renal blood supply is from the renal artery that progressively branches to form afferent arterioles and the glomerular capillaries. The distal ends of the glomerular capillaries coalesce to form efferent arterioles (Figure 4). This will lead to a secondary capillary network; the peritubular capillaries in the cortex and *vasa recta* in the medulla, surrounding the renal tubules, which in turn will empty into vessels forming the renal venous system (36).

Plasma is filtrated through the GFB from the capillaries in glomerulus into Bowman's capsule. The GFB is a biological membrane that includes a unique type of the fenestrated endothelium, the basement membrane, and the epithelial cell layer (podocytes). The podocytes together with the mesangial cells mainly provides structural support to the GFB. The GFB has a unique ability to filter great amount of water, while still having selectivity for filtration of proteins. The selectivity is based on size and charge, and is virtually impermeable to large plasma proteins (36). Albumin is the most abundant plasma protein, and although it

is small in size, its negative charge decreases its filterability. A change in the composition of the GFB can cause the smaller proteins, such as albumin, to be filtered. This can be detected in the urine (proteinuria) (reviewed in (37)).

The glomerular filtration is the first step in urine formation. Large amount of fluid is filtrated across the GFB. The glomerular filtration rate (GFR) across the GFB is determined by the formula GFR = K_f * net filtration pressure. The filtration coefficient, K_f, is made up by the hydraulic conductivity and the filtering surface of the capillaries. The net filtration pressure is determined by balance between the hydrostatic pressure and the colloid osmotic pressure, acting across the capillary membrane. GFR is kept relatively constant byautoregulatory mechanisms such as tumoglomerular feedback (TGF). The TGF depends on an anatomical arrangement called the juxtaglomerular complex (Figure 4). The complex includes juxtaglomerular cells in the walls of the afferent and efferent arterioles, and specialized epithelial cells from the initial portion of the distal tubule, called *macula densa* (MD) (36). MD cells can sense the concentration of Na^+, (and presumably Cl^-) in the tubular fluid, via the Na^+-K^+-2Cl co-transporter (NKCC2). A decrease or increase in Na^+ uptake initiates a signal from MD that elicits inverse changes in GRF, by controlling the renal arteriolar resistance (reviewed in (38)). The importance of NKCC2 found in MD, as well as in thick ascending limb of the loop of Henle, is illustrated by the strong diuresis elicited by NKCC2 inhibiting loop diuretics like furosemide (39).

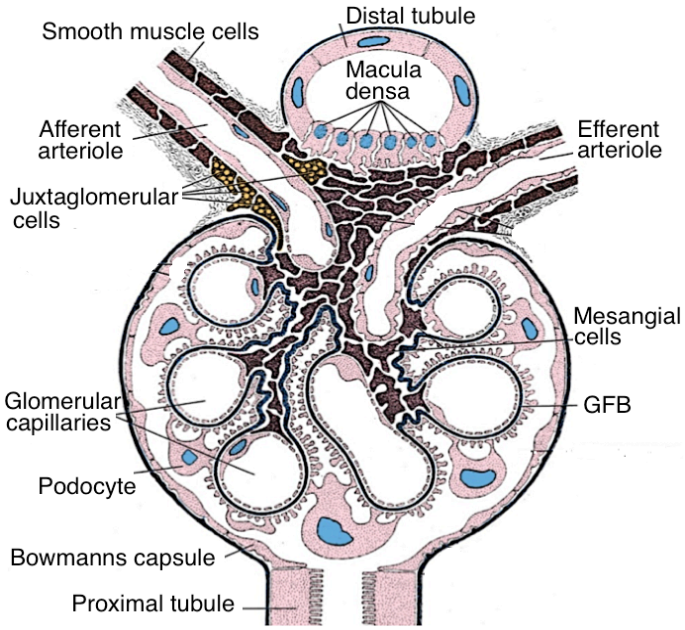

Figure 4: The structure of the renal corpsule. A schematic diagram showing the organization of the renal corpsule. The juxtaglomerular complex consists of mesangila cells associated with *macula densa* cells, and the capillary endothelium of the junxtaglomerular cells of the afferent and efferent arterioles. Figure adapted from Ros, M. H. et al. (40).

1.3.2 The renal tubules and collecting ducts

The filtrate flows from Bowman's capsule into the proximal tubules, where a substantial amount of the filtrate (water, electrolytes, sugars, amino acids, and proteins) is reabsorbed. The filtrate next enters the loop of Henle, protruding into the medulla of the kidney. In the descending loop of Henle water is lost from the filtrate through osmotic movement. In the ascending limb electrolytes are reabsorbed by active transport across the tubular epithelium (36). The loop of Henle and *vasa recta* are arranged in a counter current multiplication system, establishing a cortico-medullary osmotic gradient, neccesarry to concentrate the urine (reviewed in (41)). The following nephron segment is the distal tubule, located in the cortex. The initial portion of the distal tubule contains the short *macula densa* segment. Several distal tubules drain into each cortical collecting duct, which subsequently enters the medulla as medullary collecting duct. In the collecting duct the final water- salt- and urea reabsorption occurs. Finally, the collecting ducts merge to form the *renal pelvis*, which joins the ureter leading to the urinary bladder (36).

1.3.3 The regulation of diuresis by vasopressin

A key regulator of diuresis is the anti-diuretic hormone vasopressin (AVP). AVP was first discovered as a vasopressor (42). Later it was identified as an anti-diuretic hormone (43), and established as the primary regulator of water balance and maintenance of plasma osmolality (44). AVP is released into the blood stream in response to increased plasma osmolality or decreased circulating plasma volume. In response to a large water intake, plasma will be diluted, endogenous AVP will be suppressed, and urine produced will be more hypo-osmotic relative to blood plasma. Changes in the excretion rate of urinary solutes, such as salt and urea are, however, modest (reviewed in (41)).

Two AVP receptors isoforms exists, V1a,b mainly exerting the vasopressor effects, and V2 primarily exerting the anti-diuretic effects (reviewed in (45)). The V2 receptor (46) is predominantly located in the kidney, most abundantly in the apical membrane of collecting duct cells (47). Desmopressin (dDAVP) is a synthetic AVP analogue for the V2 receptor, and has enhanced anti-diuretic potency, and a markedly diminished vasopressor activity (48). Binding to the V2 receptor activates $G\alpha_s$ coupled to AC, that when activated generates cAMP (48). The main function of AVP through cAMP is to increase the water permeability along the entire collecting duct via regulation of the water channel Aquaporine-2 (AQP-2),

additionally it increase urea permeability in the inner medullary collecting duct via regulation of the urea transporter UT-A1 (49, 50).

The predominant AVP-regulated water channel AQP-2 (49) is essential for regulation of water balance, and is abundant in the apical membrane of the final part of the distal tubules and in the collecting duct (51, 52). AVP regulates AQP-2 mainly by enhancing its movement from intracellular vesicles to the luminal membrane of the duct cells (53). AQP-2 contains several consensus sites for PKA phosphorylation, some of which have been shown to be critical for AVP-induced trafficking and subsequent apical membrane accumulation (54, 55). In perfused inner medullary collecting ducts, pre-incubation with a substance that buffers intracellular Ca^{2+}, blocked the osmotic water permeability, indicating that intracellular Ca^{2+} is required for AQP2 membrane insertion (56). Additionally AVP leads to increased AQP-2 transcription (57). This involves the cAMP responsive element (CRE) pathway, where PKA induces phosphorylation of the cAMP response element (CRE) binding protein (CREB), which stimulates transcription via CRE in the AQP-2 promotor (58).

Urea is the predominant end product of nitrogen metabolism in mammals, and is freely filtrated in the kidney glomerulus. Urea is transported through urea transporters (UT-A,B). Reabsorption of urea in kidney inner medullary collecting duct (IMCD) by UT-A1 and UT-A3 and by UT-B1 in the *vasa recta* are predominantly responsible for urea accumulation in medullary in the urinary concentration process. This accumulation of urea in the medulla is important to generate the osmotic driving force for maximal water reabsorption and additionally permit large amounts of urea to be excreted without obligating excessive water loss. This process is independent of electrolyte transport. UT-A1 in the IMCD (50) is regulated by AVP (59). During anti-diuresis the AVP induced generation of cAMP increases the abundance of UT-A1 in the apical membrane (60, 61), in part mediated by phosphorylation of UT-A1 (59, 62). AVP has additionally been shown to increase the expression of UT-A1 (63, 64).

1.4 The proposed roles of Epac in kidney function

The kidney is one of the organs showing the highest Epac1 mRNA expression (12, 13), exhibiting different expression patterns in the various parts of the nephron (65, 66). Immunoblots from $Epac1^{-/-}$, $Epac1^{+/-}$ and WT mice show particularly high Epac1 abundance

in kidney relative to tissue from other organs (67). Epac2 expression in the kidney has been reported (66), but at very low level compared to Epac1. Members of our research group (R. Kopperud and C. Krakstad) failed to detect any Epac2, under conditions when Epac2 was detected in liver (S. Døskeland, personal communication). *In vitro* experiments have suggested a role of Epac in mediating some of the many cAMP dependent renal processes previously attributed to PKA (65, 68-74).

The possible function of Epac in the control of glomerular barrier and GFR is not understood. A study suggests that ANG II induces collagen synthesis in mesangial cells via cAMP-Epac but not PKA. The Epac specific analog 8-pCPT-2'-O-methyl-cAMP significantly increased activity of mediators in the signaling pathway, while a PKA inhibitor, did not abolish the activity (75).

In proximal tubule cells cAMP is involved in increasing the efficiency of glucose transport (76). Lee and colleagues have suggested a role of Epac and PKA in cAMP-induced increase of sodium-glucose cotransporters (SGLT) expression via extracellular-signal-regulated kinase (ERK), Ras–mitogen-activated protein kinase, using the Epac selective cAMP analog 8-pCPT-2'-O-methyl-cAMPin addition to a PKA directed analog. Additionally Both PKA and Epac also stimulated SGLT trafficking to plasma membranes via lipid rafts (77)

In the proximal tubule and thick ascending limb of Henle, elevated intracellular cAMP levels down regulate the Na^+/H^+ exchanger 3 (NHE3), responsible for reabsorption of Na^+ (reviewed in (78)). Studies done by Honegger et al. on opossum kidney cells and murine kidney slices demonstrated that Epac selective cAMP analog (8-pCPT-2'-O-methyl-cAMP), led to inhibition of NHE3 activity, as did a specific PKA analog (68). Similar results were shown by another *in vitro* study on a LLC-PK kidney cell line, using the same cAMP analogs in addition to inhibitors of PKA and Epac. It was demonstrated that exendin-4 modulation of the NHE3 activity required activation of both cAMP receptors. This was based on the observation that PKA inhibitor blocked the effect of the PKA analog, but only partially blocked the NHE3 inhibition. The same was true for the Epac inhibitor when used in combination with the analog (69).

In the collecting tubule and collecting duct the H^+-K^+-ATPase is an ion pump using energy from ATP hydrolysis to transport H^+ out of the tubules in exchange for K^+, central in the

acid-base balance. The activation of the H^+-K^+-ATPase is not fully understood, but it is likely to involve cAMP through PKA (reviewed in (79)). A PKA independent pathway has however been suggested by Laroche-Joubert el al. Stimulation of $K^{+-}H^+$-ATPase by calcitonin, increases phosphorylation of extra cellular signal regulated kinase (ERK) in a PKA independent manner. By using antibodies directed against Epac1, the stimulation of K^+-H^+-ATPase curtailed, indicating that calcitonin stimulates $K^{+-}H^+$-ATPase through cAMP activation of Epac1 and subsequent phosphorylation of ERK (65).

An essential role of cAMP in the collecting duct is to increase apical membrane abundance of AQP-2, and UT-A1. This has long been ascribed to PKA, but several *in vitro* studies have indicated Epac to be involved. Yip and colleagues have demonstrated that studies on perfused IMCD cells treated with a PKA inhibitor did not prevent the AVP-induced $Ca2^+$ mobilization, involved in AQP-2 trafficking. Furthermore the Epac selective agonist 8-pCPT-2'-O-methyl-cAMP mimicked the effect of AVP in trigging Ca^{2+} oscillations. Together this indicates that Epac is involved in the AQP-2 exocytosis (70). Additionally Epac has been implicated in long-term regulation of AQP-2. In murine immortalized cortical collecting duct cells treated with AVP. The use of two separate PKA inhibitors did not block the up regulation of AQP-2 expression, indicating a PKA independent pathway for AQP2 mRNA expression up regulation, mediated through a cAMP-responsive element in the AQP2 promoter (71). Another study conducted by Kortenoeven et al., on murine immortalized cortical collecting duct cells showed that after dDAVP incubation AQP-2 transcription were blocked by a PKA inhibitor. Following a longer dDAVP incubation AQP2 transcription remained elevated, not blocked by a PKA inhibitor. Incubation with a specific Epac activator (8-pCPT-2'-O-methyl-cAMP) increased both AQP2 abundance and transcription compared with cells that were un-stimulated. Together this suggested that PKA is involved in the initial rise in AQP2 levels after dDAVP stimulation, but not in the long-term effect of dDAVP, which may involve Epac (72).

PKA activation has demonstrated to increase phosphorylation and subsequent exocytosis of UT-A1. Frolich and colleagues has however been demonstrated that a PKA inhibitor only partially blocked the activation of urea flux induced by AVP and forskolin in Madin-Darby canine kidney cells, indicating that this activation involves a signaling pathway beside from PKA pathway (74). A second study by Wang et al. demonstrated that an Epac activator (8-pCPT-2'-O-methyl-cAMP) significantly increased urea permeability in isolated, perfused rat

IMCD cells, and significantly increased UT-A1 phosphorylation and its accumulation in the plasma membrane, via MEK (mitogen-activated growth factor)/ERK signaling pathways. Further, stimulation of Epac by adding forskolin and inhibit PKA, significantly increased urea permeability (73).

1.5 Aim of the study

The kidney show high Epac1 expression levels, and a number of *in vitro* studies have implicated Epac1 in regulation of several renal transporters and channels, and in maintaining the GFB. An animal model has been developed, were Epac1 is knocked out, allowing for *in vivo* studies. Preliminary studies conducted in the group have revealed an increased diuresis in the Epac1$^{-/-}$ mice. The present study was therefor undertaken to investigate the renal function of Epac1 by comparing Epac1$^{-/-}$ mice to their reference WT littermates during baseline conditions as well as after a per oral water load and when water loaded and dDAVP treated. This will allow for evaluation of Epac1$^{-/-}$ mice capability to dilute and concentrate urine. Under the mentioned conditions we will measure renal excretion and/or clearance of osmolytes, electrolytes, creatinine, urea, cAMP, and albumin. This will indicate the renal consequences of deletion of Epac1. Furthermore will the expression level of AQP-2 and UT-A1 be evaluated, using quantitative Reel time-PCR (qRT-PCR) and immunoblotting. Finally Epac1 possible role in GFR will be assessed by using furosemide to block the NKCC2 co-transporters in *macula densa*, and hence the vaso-regulatory feedback to afferent arteriole.

2 Materials and Methods

2.1. Chemicals

Unless otherwise stated, the chemicals used were obtained from Sigma-Aldrich (St. Louis, MO, USA) and at least of analytical grade. Special reagents or drugs are mentioned in connection with the description of the methods/experiments where they were used.

2.2 Mouse strains and handling

The mice used were kindly provided by Dr. Stein Ove Døskeland (University of Bergen, Norway). The Epac1 knockout mouse model (referred to as Epac1$^{-/-}$ mice) included in this study was bred against a C57BL/6J-BomTac genetic background. The targeted disruption of the Epac1 gene had been generated by recombinant deletion of the cAMP-binding domain. The deletions were confirmed by genotyping and immunoblotting, all done by out group (67). Epac1$^{-/-}$ mice and littermate wild-type (WT) mice were bred in the local animal facility.

The mice used in the present study were females, 3-5 months of age, weighing 20-25 g. They were housed at constant temperature (23°C) with 12-h artificial light-dark cycle. The mice were routinely caged in groups of two to four in cages with individually ventilated cage systems, and were provided with standard rodent chow (Special Diet Services RM1, 801151, Scanbur BK, Oslo Norway) and water *ad libitium*. The animal protocols were approved by The Norwegian Animal Research Authority and performed according to the European Convention of the Protection of Vertebrates Used for Scientific Purposes. Details of animal handling are described together with the relevant experiments.

2.3 Description of the animal studies related to diuresis control

2.3.1. Overview

The animal experiments were designed to investigate the possible role of Epac1 in the diuresis. Two experimental groups of mice were included, series 1 (7 Epac1$^{-/-}$ and 6 WT mice), and series 2 (8 Epac1$^{-/-}$ and 8 WT mice). All experiments were conducted in individual MMC10 metabolic cages, specifically designed for use with mice (Hatteras Instruments, Inc, NC, USA; Figure 5A).

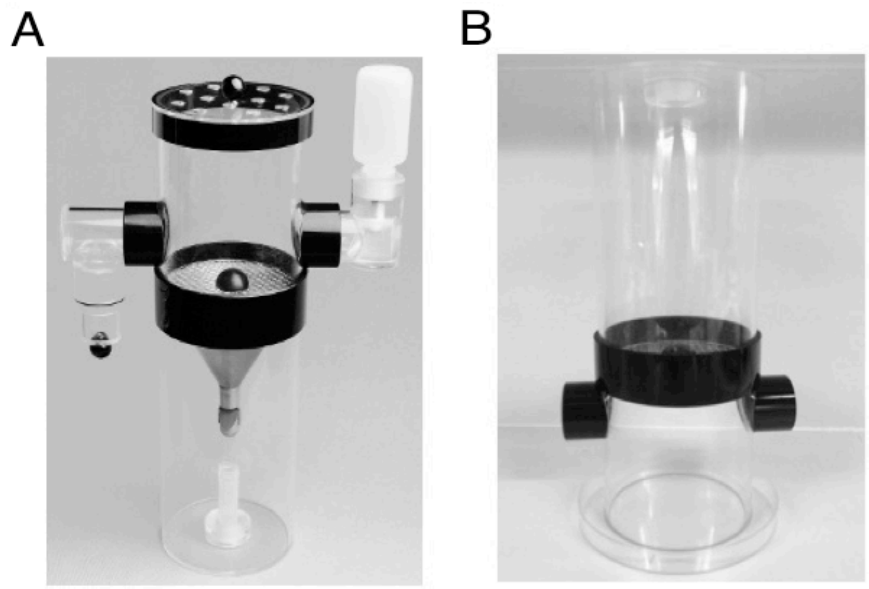

Figure 5: The individual metabolic cage. (A) The mice have free access to food from the tube on the left side of the cage, and water, from the water bottle on the right side. They stayed on top of the grid, with a funnel separating feces from the urine. Urine was collected in the tube underneath. **(B)** To conduct the continuous urine measurements the cages were slightly modified. The bottom cylinders were situated on top of the cage, with the grid in between, a siliconized petri dish were placed underneath enabling pipetting of urine as it was excreted.

Series 1 and 2 of WT (n = 14) and Epac1$^{-/-}$ mice (n = 15) were kept in the individual metabolic cages for two constitutive 24-h periods (with free access to water and food). In the first 24 h animals were adapted to the metabolic cages. In the second 24-h period diuresis and urine production were determined. They stayed in ordinary cages for one week before being used for further experiments. Following all experiment urine samples were collected, and after the latter experiment plasma samples and kidneys were collected, for further analysis. The experiments for series 1 and 2 of animals are overviewed in Figure 6 (the first 24-h period adapting the mice to the individual metabolic cages is not included).

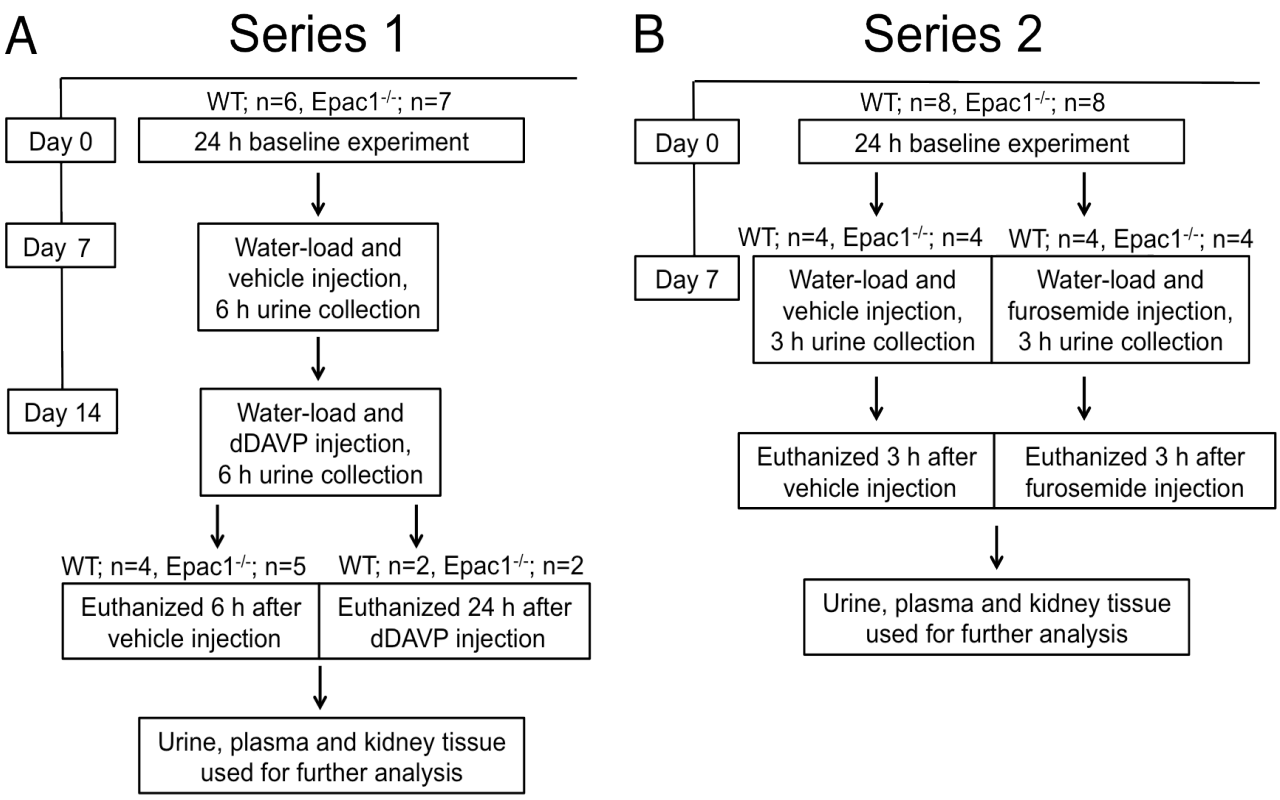

Figure 6: Overview of the animal experiments. **(A)** Series 1 of WT (n = 6) and Epac1$^{-/-}$ mice (n = 7) were included in 24-h baseline experiment. After 7 days in the ordinary cages the animals were anesthetized, water loaded (by intragastric infusion of 1.5 ml water), and injected intra-peritoneal (i.p.) with vehicle (0.9% NaCl), urine were collected in 6 h. After additional 7 days mice received water load combined with an i.p. dDAVP injection, urine were collected in 6 h. A part of the mice (n = 4 WT, n = 5 Epac1$^{-/-}$) were euthanized 6 h after dDAVP injection, the rest (n = 2 WT, n = 2 Epac1$^{-/-}$) were euthanized 24 h after dDAVP injection. Plasma and kidneys were collected. Urine, plasma and kidney tissue were analyzed. **(B)** Series 2 of WT (n = 8) and Epac1$^{-/-}$ mice (n = 8) were included in 24-h baseline experiment. After 7 days in the ordinary cages the animals were anesthetized, water loaded. Additionally half of the mice (n = 4 WT, n = 4 Epac1$^{-/-}$) were injected i.p. with vehicle, and the remaining half received an i.p. injection of furosemide. Urine was collected in 3 h, and plasma and kidneys were collected. Urine, plasma and kidney tissue were analyzed.

2.3.2 Determination of water consumption and urine output

After mice were adapted to the individual metabolic cages, the urine collecting tubes and water bottles were weighed. This was done immediately before placing the animals back in the individual metabolic cages, and after the animals had been in the cages for 24 h (Figure 5A). Urine output and water consumption was estimated as the difference in weight of the urine collecting tubes and the water bottles, respectively. The urine samples were frozen on -20°C for further analysis, and the animals were returned to the original cages.

2.3.3 Water loading, injection of dDAVP, furosemide, and continuous urine collection

In order to minimize the bladder urine content the animals were deprived of water 1 h prior to each experiment, and their urine bladders were emptied by bladder massage. The animals

then were anesthetized with Isoba® vet isoflurane (Schering-Plough Animal Health, Elkhorn, NE), followed by intra-peritoneal (i.p.) injection of 0.1 ml of either vehicle (0.9% NaCl), the AVP analog dDAVP (1 ng/g body weight), or furosemide (40 μg/g body weight), all in 0.9% NaCl. A few seconds after the i.p. injection each animal received 1.5 ml water by intragastric intubation through a 38 mm metal feeding needle with a silicon tip (AgnTho's AB, Sweden). Immediately thereafter the mice were placed in the individual metabolic cages, slightly modified with a siliconized inset (Figure 5B) to facilitate the quantitative recovery of the spontaneously voided urine. The time point of each excretion was noted, and its volume determined by pipetting urine from the siliconized petri dish placed underneath the cage into a pre-weighed tube. These data were used to construct the urinary output as a function of time after the onset of the experiment (defined as the time point when the bladder was emptied after massage). The urine samples from individual animals were frozen on -20°C for further analysis. In the experiment conducted to series 1 of mice (receiving vehicle, or dDAVP injection) urine were collected for 6 h (Figure 6A). The experiment conducted to series 2 of mice (receiving vehicle, or furosemide injection), urine was collected for 3 h (Figure 6B). A shorter time for collection were performed in this experiment to minimize possible secondary effects of furosemide.

2.3.4. Sampling and preparation of blood and kidney tissue for subsequent analyses

The animals were euthanized with CO_2 gas, 0.4 ml blood was rapidly aspirated by cardiac puncture into a 0.5 ml syringe with 0.1 ml Anticoagulant Citrate-dextrose solution, and centrifuged for 3 minutes at 500 rpm in an Eppendorf mini-centrifuge to yield plasma. Plasma samples was stored at –20°C together with urine samples until assayed. The kidneys were quickly removed, sliced horizontally and each half quickly cut into smaller pieces before being flash-frozen in liquid nitrogen and stored at -80°C.

Total RNA was isolated using the TRIzol reagent according to the manufacturer`s protocol. Briefly, 100 mg frozen kidney tissue was homogenized as described for protein extraction, except that the extraction medium was TRIzol. After washing and drying, the pellet containing total RNA was dissolved in 0.1 ml of 0.2 % diethyl pyrocarbonate-treated water. The RNA concentration was estimated using the Nano-Drop® Spectrophometer ND-1000, (Saveen Werner, Limhamn, Sweden). All samples were run on a 1 % agarose gel and 18S and 28S ribosomal RNAs visualized by standard ethidium bromide staining. Visual

inspection of the staining patterns revealed a close correlation between the intensity of the 28S and 18S bands and the spectrophotometrically determined concentrations in each sample.

For protein extraction for subsequent western blot analysis tissue from one kidney half (about 0.1 g) was homogenized, while still frozen, in ice-cold 50 mM Tris (pH 7.4) buffer with 150 mM NaCl, 0.5 % Sodium deoxy-cholate, 1 % tergitol-type nonyl phenoxypolyethoxyl-ethanol-40 (NP-40), 0.1 % Sodium dodecyl-sulfate (SDS), with Protease Inhibitor Complete (Roche Diagnostics GmbH, Germany) added according to the manufacturers' protocol, using two cycles of 20 seconds at maximum speed of a Heidolph DIAX 900 homogenizer. The samples were incubated at room temperature for 30 min, before centrifuged at 2900 X g for 20 min at 4°C (Biofuge Stratos, Heraeus, Thermo Electron Corporation, Germany)**.** The amount of protein in each sample was measured using the Bradford method (Bio-Rad Protein assay Kit II, Bio-Rad Laboratories, Hercules, CA, USA) with bovine serum albumin (BSA) as standard. The absorbance was measured at 575 nm using an ASYS UMV340 plate reader (Biochrom, Cambridge, UK).

2.4 Methods used to analyze urine, plasma, and kidney tissue

2.4.2 Quantitative Real time PCR

To determine relative AQP-2 and UT-A1 mRNA levels by quantitative real time- PCR (qRT-PCR) 1.5 µg total kidney RNA was first reverse transcribed to cDNA by PCR in a mixture with 0.75 µM random hexamer and 1.5 µM Oligo-dT primer, 1 mM dNTP-mix and 50 U RevertAid Reverse Transcriptase (Thermo Scientific, USA). The PCR was preformed for four cycles with following conditions: 25°C for 10 min, 42°C for 60 min, 70°C for 10 min and 4°C forever (MJ Research PTC-200 Peltier Thermal Cycler, Bio-Rad Laboratories, Hercules, CA, USA). The qRT-PCR was carried out using cDNA corresponding to 5.5 ng RNA. Two repeated qRT-PCR runs, using the same cDNA were conducted. cDNA was added to a master mix, containing 1x iQ TM SYBR® Green Supermix (Bio-Rad Laboratories, Hercules, CA, USA) and 0.2 µM of each of the primers. The primer sequences used were: AQP2, sense 5`-GCCCTGCTCTCTCCATTG-3` and antisense 5`-TCAAACTTGCCAGTGACAAC-3`; UT-A1, sense 5`-CTGCCACCTGGGCTTCTTTTG-3` and antisense 5`-GGGTAACGCCTGAGAGACAAG-3`. The amplification signals were normalized to tree unrelated reference genes: succinate dehydrogenase complex subunit alpha (SDHA) mRNA levels, sense 5`-CATGCCAGGGAAGATTACAA-3` and antisense 5`-

GCACAGTCAGCCTCATTCAA-3`, Ppia mRNA level, sense 5`-TGAGCACTGG-AGAGAAAGGA-3`, and anti sense, 5`-CCATTATGGCGTGTAAAGTCA-3` and cGMP-dependent protein kinase (Pkg1) mRNA level, sense 5`- TGGATGACGTTTCCAACAAA-3`, and anti sense, 5`-CACTATGTGGCGCTTCTTGA-3`. Total volume was adjusted with MQ. PCR amplification was carried out on a 384 well PCR plate, in the LightCycler 480 II (Roche, Basel, Switzerland). The following set of cycles were performed; 1 cycle for 300 sec at 95°C (pre- incubation), and 40 cycles for 10 sec at 95°C, 10 sec at 60°C and 20 sec at 72°C (amplification).

2.4.1 SDS-PAGE and Western Blot analysis

AQP-2 and UT-A1 protein level were determined by sodium dodecyl sulfate-polyacrylamide gel electrophoresis (SDS-PAGE) and western blot. SDS-PAGE was employed to separate denatured proteins by size. Kidney extract aliquots (see section 2.3.4) containing 0.2 mg protein was mixed with equal volumes of sample buffer (0.25 M Tris-HCl, pH 6.8, 2 % SDS, 20 % glycerol 5 % mercaptoethanol), heated at 60°C for 10 min, and thereafter at 95°C for 5 min. After cooling, the samples were separated on a 4 % to a 12.5% linear gradient reducing SDS-polyacrylamide gel. The gels were run at 120 volts. The running buffer was 0.25 M Tris, 1.92 M glycine, 0.5 % SDS (pH 7,5). The polypeptides separated by the SDS-PAGE, including the pre labeled "Precision Plus Protein Standard All Blue" (BioRad Laboratories, Hercules, CA, USA) proteins were transferred from the gel to a polyvinylidene difluoride membrane (GE Health- care Life Sciences, Buckinghamshire, UK) electrophoretically, in blotting buffer (25 mM Tris, 190 mM glycine, 20 % methanol, pH 8.3), in a Transphor Electrophoresis unit (Hoefer Scientific instruments, San Francisco, CA, USA). The transfer was run at 200 mA for about 16 h, while kept cool by a Pharmacia LKB Multi Temp cooling loop (Pharmacia LKB Biotechnology, Sweden) with constant running buffer agitation (by a magnetic stirrer).

After blotting, the membranes were washed in a PBS-Tween solution (PBS containing 5 mM $MgCl_2$ and 0.04 % (v/v) Tween20), and nonspecific antibody binding sites blocked in blocking buffer (0.05 M TBS containing 0.16 % (v/v) I- BlockTM (TROPIX, Applied Biosystems, MA, USA), 0.02 % (v/v) Na N_3, 4 mM $MgCl_2$ and 0.02 % (v/v) Tween20) for 1 h. The blots were next probed with primary antibody diluted in blocking buffer for 18 h at 4°C with gentle agitation. The primary rabbit anti-AQP2 antibody, kindly provided by Prof.

Robert A. Fenton, University of Aarhus, Denmark, was used in a 1:3000 dilution. The probed membranes were washed thoroughly in PBS-Tween solution, and incubated with secondary goat anti-rabbit IgG antibody, coupled to alkaline phosphatase, at 1:10 000 dilution.

The membranes were next washed to remove any unbound secondary antibody and incubated in 100 mM diethanolamine with 100 mM $MgCl_2$ pH 9.5 for 2 x 2 min before adding the alkaline phosphatase substrate; CDP-star (Tropix; Bedford, MA, USA) according to the manufacturers' protocol. The immunoblots were visualized with a Fujifilm LAS-3000 chemiluminescence detection system (Fujifilm, Tokyo, Japan) and the intensity of the blotted bands quantified by densitometry using the software Multi Gauge volume 2.3. Endogenous β-actin served as loading control, membranes stripped in 0.5M Tris-HCl pH 6.7 with 10 % (v/v) SDS and 0.1 % (v/v) mercaptoethanol for 10 min, and washed in blocking buffer. The membranes were then incubated in anti-β actin antibody (1:10 000) (Abcam, UK) for 16 hours and the remaining protocol was performed as described.

2.4.3 Urine and plasma osmolality and electrolyte analysis

The osmolality in individual urinary and plasma samples was measured using a Wescor 5500 vapor pressure osmometer (Wescor Inc., Logan, Utah, USA) according to manufacturer's protocol. Briefly, filter paper discs (SS-033 Wescor Inc., Logan, Utah, USA) were placed on the sample holder, and 10 µl urine sample added. Urine at base line was diluted two fold before applied, while urine samples from the other experiments were applied undiluted. Three reference solutions (50, 290 and 580 mOsm; Wescor Inc., Utah, USA) were used for calibration. Additionally the urine electrolytes (Na^+ and K^+) were determined by routine ion-selective electrode techniques in 0.5 ml urine sample (Analyzed by the Laboratory for Clinical Biochemistry at Haukeland Hospital in Bergen, Norway).

2.4.4 Urine and plasma urea and Creatinine determination

The urea concentration was determined in urine and plasma using the QuantiChrom™ *Urea* Assay Kit (DIUR-500; BioAssay systems, Hayward, CA, USA). The assay was conducted using a 96-well plate procedure, and the absorbance was measured at 520 nm using the ASYS UMV340 plate reader. The kit was used according to the manufactures protocol, with some alterations. The volume standard and sample were increased from 5 to 25 µl for a more precise determination. A highly reproducible standard curve was made. The urine samples

were diluted according to their concentration, ranging from 100- to 50-fold. The plasma samples had to be partially deproteinized to obtain reliable estimates. For this the plasma samples were diluted 5-fold in MQ water and filtered through centrifugal filter units with Ultracel-30 membrane with a nomical cut-off of MW 30,000 (Millipore, Billerica, MA, USA) by centrifugation (Biofuge Stratos, Heraeus, Thermo Electron Corporation, Germany) at 5000 rpm for 10 min at 4^{o}C. Importantly, the unfiltered plasma quenched the color reaction from added urea (not shown).

Urine creatinene was analyzed by the Laboratory for Clinical Biochemistry at Haukeland Hospital in Bergen, Norway. It was determined in a 0.5 ml sample, by an enzymatic creatinase assay (CREA Plus kit; Boehringer Mannheim, Indianapolis, IN), using a Roche Cobas Bioanalyser (Roche, Nutley, NJ). Due to a limited amount of plasma available for analysis, the concentration of creatinine in plasma was determined separately. T The method was based on a method described by Haselene-Hox et al. (80), but with some modifications. Plasma samples (10 μl) were deproteinized by adding 10 μl 10 % trichloracetic acid, before centrifuging at 20 000 X g for 10 min to remove precipitated proteins. Supernatant (15 μl) was injected onto a 2D-HPLC system equilibrated with 20 mM sodium acetate buffer (pH 4.68). Creatinine, which is positively charged at pH 4.68, was separated from trichloracetic acid and other interferents in the first dimension column (1 ml Resource S, GE Healthcare, UK). By switching to 10 mM Potassium buffer (pH 7.10) in the second dimension column (Proswift SCX-1S, 4.6x50 mm, Dionex, Sunnyvale, CA) the creatinine molecule was neutralized, resulting in a reduced retention and a sharp, well-defined peak detected at its absorption maximum of 234. The specificity of the method was validated by analysis of urine and plasma samples before and after treatment with creatininase (EC 3.5.2.10, 1000 U) and by creatinase (EC 3.5.3.3, 500U) at 25°C overnight with 13 U/ml and 30 U/ml of creatininase and creatinase, respectively.

2.4.5 Calculations of clearance and fractional clearance, and free water clearance

By definition plasma to urine clearance (C) of a given substance x is the volume of plasma completely cleared of this substance per unit of time, and is resolved by determining the substance concentration in urine and plasma, and relating it to the diuresis ($\dot{V}$; µl excreted per min), using the formula:

$$C_x = \frac{Urine_x}{Plasma_x} \times \dot{V}$$

Accordingly, the clearance of creatinine, urea, Na^+, K^+ as well as for osmolytes was calculated. A feasible parameter for evaluating urinary diluting and concentrating activity is to calculate the "solute-free water clearance" or "free water clearance", and it was calculated using the following formula:

$$\text{Free water clearance} = \dot{V} - C_{Osmo}$$

The creatinine clearance was assumed to be equal to the glomerular filtration rate (GFR), as the amount filtered is almost equal to the amount excreted. By relating the clearances of the substance x to the creatinine clearance, it gives an impression of the renal handling of the substance x. It will provide the percent of the filtered substance that is excreted in the urine. The fractional clearance of osmolytes, Na^+, K^+ and urea was calculated according to the formula:

$$\text{Fractional clearance} = 100\% \times \left(\frac{C_x}{C_{Creatinine}}\right)$$

2.4.6 Determination of proteinuria

Accumulation of proteins in the urine is a key feature of renal disease, and a consequence of an impaired glomerular filtration barrier. Some degree of proteinuria in the Epac1$^{-/-}$ mice could indicate that Epac1 is involved in maintaining the selectivity of the GFB. Albumin in urine and in plasma was determined by 2D-HPLC using a size-exclusion chromatography in the first dimension and reversed phase chromatography in the second dimension. This was performed in collaboration with Prof. Olav Tenstad (Dept. Biomedicine, Med. Faculty, Univ. of Bergen). Undiluted urine (10 µl) or Plasma diluted 1:100 in phosphate buffer (0.1 M Na_2SO_4, 0.05 M HNa_2PO_4, 0.05 M H_2NaPO_4, pH 6.8) was injected onto the first dimension column (Super SW2000, 4.6 x 300 mm, Tosoh Bioscience, Tokyo, Japan) and separated from IgG and other larger plasma proteins. The albumin fraction was automatically loaded onto the second dimension column (Proswift Rp4H 1 x 50 mm, Dionex, Sunnyvale, CA) at a flow rate of 0.35 ml/min by an inline switch. Albumin was then separated from proteins with similar

molecular weight by an eight-minute acetonitrile gradient (5–60 %). The albumin concentration was determined based on the area under the curve for standards and samples (81).

2.4.7 Determination of urinary cAMP

The urinary samples were diluted according to their concentration in 0.1 M HCl and 0.1 M CH_3COOH, neutralized with 0.5 M Tris base containing 0.5 M NaOH, 0.1M Na_3PO_4, and 40 mM EDTA to pH 7.2.

The cAMP concentration of the urinary samples was determined by an assay based on competitive displacement of [^{3}H]cAMP by cAMP from binding to site B of the RIα subunit of PKA type I. The assay is an improved version of one using salt-dissociated PKA type I (82). Instead of dissociating the PKA holoenzyme into free cAMP binding R subunit and catalytic C subunit to improve the cAMP affinity of the R subunit we used here the free RIα subunit alone, produced from recombinant cDNA and expressed in E. coli. Since each RIα subunit has two cAMP binding sites (low affinity site A and high affinity site B) we used a RIα subunit whose A site had been inactivated by mutation (RIα G201E) so that only the B site can bind cAMP. This method gave a highly sensitive detection of cAMP, allowing the cAMP level to be reliably detected even at the low concentrations in the highly diluted urine samples from water-loaded furosemide treated animals (82, 83).

Details of the assay are as follows: the [^{3}H] labeled cAMP ([2,8-3H]Adenosine3′5′cyclic phosphate, Amersham Biosciences, UK; 27 Ci/mmol) was diluted in 40 mM Hepes, 40 mM TrisHCl, 20 mM EDTA, 2 mM EDTA, pH 7.4 to 4.8 nM [^{3}H]cAMP. An aliquot (60 µl) of this solution was mixed with the sample (120 µl) and next with 60 µl of 2 nM RIαG201E in a pH 7.4 buffer containing 40 mM Hepes, 40 mM TrisHCL, 20 mM EDTA, 2 mM EGTA, 1 mM TCEP, 0.1 mM IBMX, 2 mg/ml of BSA and 1 mg/ ml of soybean trypsin inhibitor. After thorough, but careful mixing of their contents the reaction vials were incubated on ice in a cold-room for 16 h.

At the end of incubation duplicates of 100 µl were removed and mixed with 3 ml ice-cold aqueous 3.8 M ammonium sulfate. The precipitate is collected on Millipore cellulose ester filters (0.3 µm pore size) (Microcon YM-10, Amicon, Beverly, MA, USA) by vacuum

filtration (Model 1225 Sampling Manifold, Millipore Corp., Bedford, MA, USA). The filters were washed twice with 65 % saturated ammonium sulfate solution, transferred to counting vials containing 3 ml of aqueous SDS (2 % W/v), mixed vigorously on a vortex mixer, added 10 ml of water-compatible scintillation liquid (Emulsifier-safe ™, Perkin-Elmer, Inc., Waltham, MA, USA), before vortexed again. The amount of added isotope was determined by adding 60 µl of 4.8 nM [^{3}H]cAMP directly to scintillation vials. In order to ensure similar quenching of radioactivity as for the assay samples these vials contained 2.94 ml of the 2 % SDS solution and a "mock" filter treated like the others. The vials were left for a couple of hours in the dark before being transferred to a scintillation counter and counted for 10 minutes. The radioactivity was determined by scintillation counting in a Tri-Carb 2900TR Liquid Scintillation Analyzer (Perkin-Elmer, Inc., Waltham, MA). The amount of cAMP in each sample was determined based on the amount of [^{3}H]cAMP displaced from RIα as compared to standards with known cAMP concentration.

2.10 Graphic illustration and statistical analysis

Excel 2014 (Microsoft Corporation, Seattle, WA, USA) was used for graphic illustrations and statistical calculations (SEM, Student T-test). Data sets are generally presented as means ± SEM. For comparison of variables in Littermate animals relative to the Epac1$^{-/-}$ animals, statistical significance was assessed by a two-tailed unpaired Student *t*-test. P values ≤ 0.05 were the criterion for statistical significance.

3 Results

3.1 The diuresis in Epac1$^{-/-}$ mice

Epac1$^{-/-}$ animals were subjected to baseline experiments, to investigate the possibility of a role of Epac1 in diuresis control. For this, the first series of WT (n = 6) and Epac1$^{-/-}$ mice (n = 7) were hosted for 24 h in individual metabolic cages with free access to water and food (see Figure 6A in methods section fro work flow). The urine produced during this period was collected quantitatively and analyzed. The consumption of drinking water was also determined. The findings are presented in Table 1A together with the body weight of the animals. A significant increase in diuresis was observed in the Epac1$^{-/-}$ relative to WT animals. In accordance with the higher diuresis, Epac1$^{-/-}$ animals had increased water consumption and decreased urine osmolality, although not statistically significant. No differences were observed between WT and Epac1$^{-/-}$ mice in Na^+ and K^+ excretion, nor in urea- and creatinine excretion.

Table 1: Weight, water consumption, urine output, urine osmolality, and Na^+, K^+ urea and creatinine excreted by Epac1$^{-/-}$ mice.

Variable determined	WT mice (n = 6)	Epac1$^{-/-}$ mice (n = 7)	P-value
Body weight (g)	20.3 ± 0.70	20.7 ± 0.78	0.71
Water consumption (ml)	2.72 ± 0.662	6.03 ± 1.527	0.11
Urine output (ml)	1.52 ± 0.296	3.72 ± 0.905	0.04
Urine osmolality (mOsmol/kgH_20)	1773 ± 285	1215 ± 223	0.17
Urine Na^+ (μmol/min)	0.16 ± 0.041	0.14 ± 0.042	0.76
Urine K^+ (μmol/min)	0.17 ± 0.022	0.19 ± 0.062	0.73
Urine urea (mmol/min)	1.27 ± 0.104	1.30 ± 0.163	0.92
Urine creatinine (nmol/min)	1.49 ± 0.232	2.25 ± 0.671	0.31

WT (n = 6) and Epac1$^{-/-}$ mice (n = 7) were weighed and transferred to metabolic cages for 24 h. During this period water consumption and urine output were determined. The urine was analyzed for content of Na^+, K^+, urea, and creatinine. Based on these parameters their average excretion rate (per min) during 24 hours was determined. Values are presented as means ± SEM.

When 8 additional WT and Epac1$^{-/-}$ mice were studied under identical conditions (the series 2 of mice, see Figure 6B in methods section fro work flow), to those included in Table 1A the same trend was found. The mean values of all WT (n = 14) and Epac1$^{-/-}$ mice (n = 15) showed that the weight still was the same (WT; 21.2 ± 0.63 g vs. Epac1$^{-/-}$; 21.0 ± 0.82 g). The difference in urine output became more significant (WT; 1.35 ± 0.136 vs. Epac1$^{-/-}$; 3.37 ±

0.427, P < 0.01), and the difference in water consumption became statistically significant (WT; 3.66 ± 0.662 vs. Epac1$^{-/-}$; 5.90 ± 0.780, P = 0.03). Urine from this experiment was not analyzed.

To further evaluate the urine concentrating capacity, the first series of WT (n = 6) and Epac1$^{-/-}$ mice (n = 7) were used, 7 days after the 24-h baseline experiment. The mice were water deprived for 1 h, and urinary bladders were emptied, by bladder massage. This was done to minimize any variations in water-intake among the animals. Subsequently the mice were subjected to a 1.5 ml oral water load. In addition to the water load the mice also received an i.p. injection of 0.1 ml of 0.9 % NaCl (because the same series of mice, after another 7 days of acclimatization, were subjected to a second water loading experiment where they received a dDAVP injection in 0.9 % NaCl, as described in section 3.2, see Figure 6 for work flow). During the following 6 h stay in the individual metabolic cages, urine was collected as it was voided. Already after about 1.5 h the injected water load was excreted (Figure 7). Only from this time point did a difference in total excreted volume between WT and Epac1$^{-/-}$ mice appear, a difference that was statistically significant 5 h after water loading. The total volume excreted was 2.16 ± 0.071 ml in WT against 2.54 ± 0.111 ml in Epac1$^{-/-}$ animals (P = 0.02).

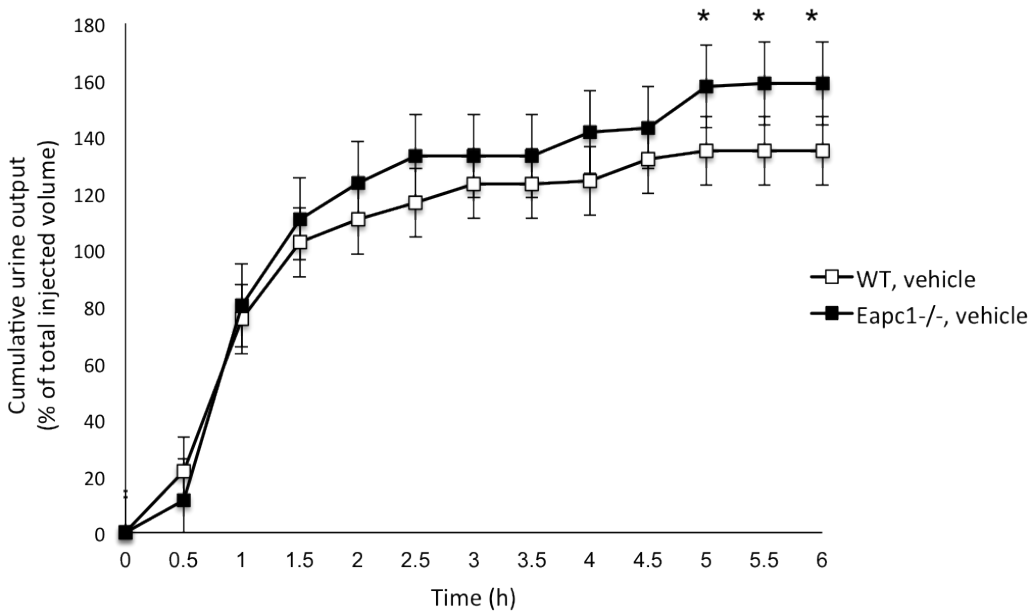

Figure 7: The diuretic response of Epac1$^{-/-}$ mice to water loading. The WT (n = 6) and Epac1$^{-/-}$ animals (n = 7) used in the baseline experiment (see Table 1A) were 7 days later subjected to water loading and vehicle injection, followed by a 6 h continuous urine collection in individual metabolic cages. Data are expressed as cumulative urine excretion, as percentage of the loaded water volume (1.6 ml). Values are means ± SEM, *P < 0.05 vs. WT

3.2 Vasopressin induced anti-diuresis in Epac1$^{-/-}$ mice

The increased diuresis of the Epac1$^{-/-}$ animals prompted a study of their response to the V2 receptor selective vasopressin (AVP) analog desmopressin (dDAVP). The water loading experiment was therefore repeated on the same first series of WT (n = 6) and Epac1$^{-/-}$ animals (n = 7) after another 7 days of acclimatization, but now adding dDAVP to the i.p. injection (1 ng/g body weight). In this way each mouse was used as its own control, regarding the effect of dDAVP. One of the Epac1$^{-/-}$ mice did not excrete measurable quantities of urine. This was due to technical problems, and consequently, this animal was excluded from the analysis. For the remaining animals the following 6 h, continuous urine collection revealed a strong anti-diuretic effect of dDAVP, overpowering the effect of the acute water load in both WT and Epac1$^{-/-}$ animals (Figure 8). The results from the previous water loading experiment are also included in the figure to visualize the relative dDAVP effect. The dDAVP-induced reduction in 6 h urine output after water loading was 49.42% in WT (2.16 ± 0.07 vs. 1.09 ± 0.13 ml, P < 0.01) and 47.51% in Epac1$^{-/-}$ mice (2.54 ± 0.113 vs. 1.33 ± 0.133 ml, P < 0.01). The difference in total diuresis between the WT and the Epac1$^{-/-}$ mice was not statistically significant (P = 0.126).

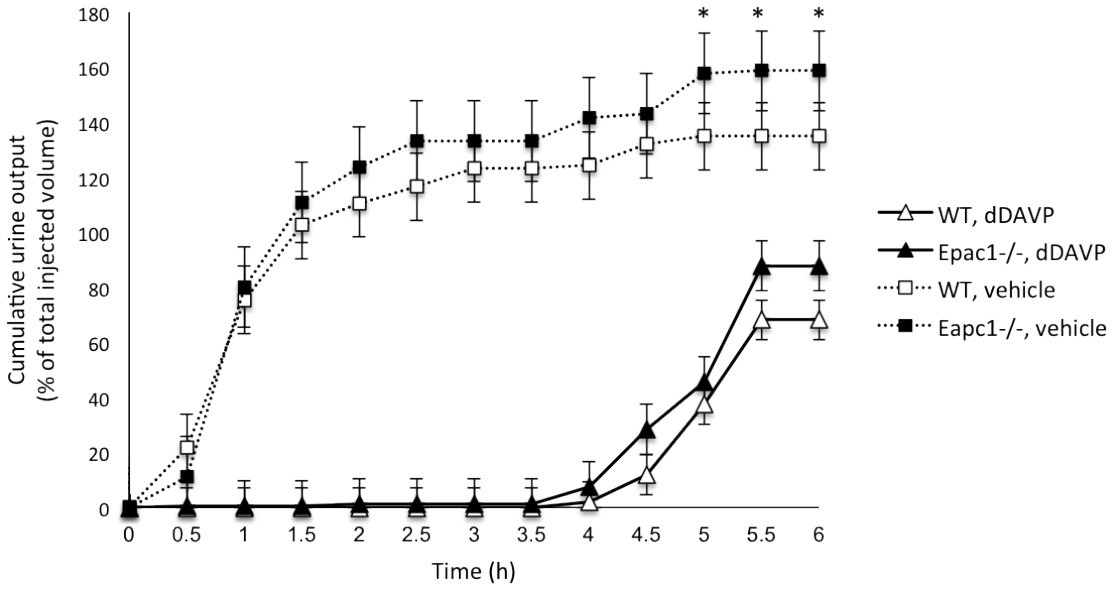

Figure 8: Epac1$^{-/-}$ mice diuretic response to water loading ± dDAVP treatment. The same series of WT (n = 6) and Epac1$^{-/-}$ animals (n = 6) as in Figure 7 were, after 7 days, subjected to water loading and a dDAVP injection. This was followed by a 6 h continuous urine collection while mice were kept individual metabolic cages. The results from the water loading experiment were included in the figure to illustrate the relative effect of dDAVP. Data are expressed as cumulative urine excretion as percentage of the loaded water volume (1.6 ml). Values are presented as means ± SEM, *P < 0.05 vs. WT

Urine samples from WT (n = 6) and Epac1$^{-/-}$ mice (n = 6) included the two water loading experiments, and plasma samples collected following the latter experiment, were further analyzes.

Urine osmolality is in addition to urine flow, the most immediate parameter for evaluating the response to AVP. The anti-diuretic effect of dDAVP treatment was accompanied by a highly significant increase in urine osmolality relative to urine collected after water loading ($P < 0.01$) in both WT and Epac1$^{-/-}$ mice (Figure 9A). While no difference in osmolality could be detected after water loading (WT; 249 ± 7.4 mOsmol/kgH_2O vs. Epac1$^{-/-}$; 233 ± 14.9 mOsmol/kgH_2O, $P = 0.3$), osmolality was significantly lower in Epac1$^{-/-}$ mice relative to their WT littermates, following dDAVP injection (WT; 589 ± 58.4 mOsmol/kgH_2O vs. Epac1$^{-/-}$; 443 ± 33.5 mOsmol/kgH_2O, $P = 0.05$). Figure 9B displays the increase in osmolality in response to dDAVP treatment in individual animals. Epac1$^{-/-}$ mice revealed a significantly smaller increase in osmolality in response to the dDAVP treatment (WT; 163 ± 35 % vs. Epac1$^{-/-}$; 77 ± 11 % $P = 0.02$).

The osmolar clearance, the fraction of osmolytes filtered from plasma that is excreted in the urine, was not significantly different in WT and the Epac1$^{-/-}$ mice under any of the experimental conditions (Figure 9C). Free water clearances were as expected positive for water-loaded animals, as urine excreted was hypo-osmotic to plasma (Figure 9D). When treated with dDAVP along with the water load the induced anti-diuresis caused the urine excreted to be hyperosmotic to plasma, and free water clearance became negative. Hence, a significant decrease in free water clearance ($P < 0.01$) was observed both in WT and Epac1$^{-/-}$ animals. Additionally the results demonstrated that Epac1$^{-/-}$ mice had a significantly higher (less negative) free water clearance in response to dDAVP (WT; -2.00 ± 0.213 vs. Epac1$^{-/-}$; 1.06 ± 0.251, $P < 0.02$). Thus Epac1$^{-/-}$ mice excreted less concentrated urine, relative to their WT littermates following the dDAVP treatment.

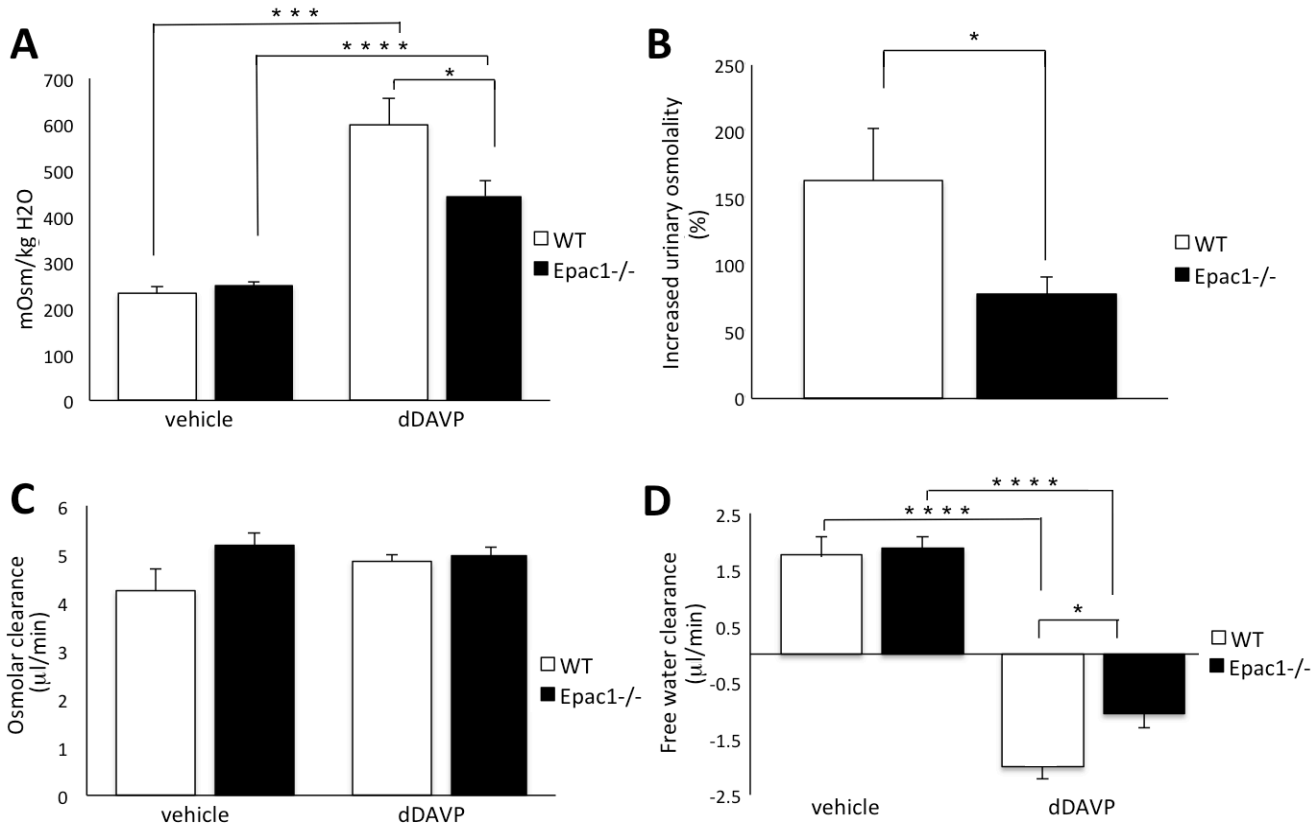

Figure 9: Osmolality of Epac1$^{-/-}$ mice urine and plasma samples, the effect of dDAVP. Urine osmolality determined in individual urine samples from WT (n = 6) and Epac1$^{-/-}$ mice (n = 6) collected in 6 h after water loading, and next after mice was treated with dDAVP in combination with the water load. Plasma samples were collected following the last experiment. **(A)** Osmolality (mOsm/kg$H_2$0). **(B)** The increase in osmolality in response to dDAVP treatment in individual animals. **(C)** Osmolar clearance (µmol/min). **(D)** Free water clearance (µmol/min). Values are presented as means ± SEM, **P* < 0.05, *** P < 0.001, ****P < 0.0001.

3.2.1 Solute excretion, and fractional clearance in Epac1$^{-/-}$ mice, the effect of dDAVP

The moderately reduced ability of the Epac1$^{-/-}$ mice to conserve water in response to dDAVP might be explained by perturbed medullary vasopressin-induced urea reabsorption. This could be reflected by altered fractional urea clearance, determined by relating the clearance of urea to the creatinine clearance (see Methods, section 2.4.5 for calculations). The fractional clearance was additionally evaluated for osmolytes, Na^+ and K^+.

To test this hypothesis, urine samples were analyzed for content of creatinine, urea, Na^+ and K^+, in addition to the osmolality analyses done. The plasma was analyzed for osmolality and content of creatinine and urea, to estimate the urinary clearance. The plasma values for Na^+ and K^+ are according to the literature considered to be quite stable at 140 mM, and 5 mM, respectively. Plasma values used to determine creatinine clearance values are mean values for WT and Epac1$^{-/-}$ mice (WT; 4.9 mM vs. Epac1$^{-/-}$; 4.3 mM).

The urinary secretion of creatinine (Figure 10A), osmolytes (Figure 10C), Na+ (Figure 10E), K^+ (Figure 10G), and urea (Figure 10I) revealed to be higher in water-loaded Epac1$^{-/-}$ than WT mice. The increase was statistically significant (P = 0.03) for osmolytes, Na^+, and K^+.

Epac1$^{-/-}$ mice showed a significant increase in creatinine excretion in response to dDAVP administration (Fig 10A). Surprisingly, the creatinine clearance was significantly higher in Epac1$^{-/-}$ mice during water loading (WT; 396 ± 45.0 μmol/min vs. Epac1$^{-/-}$; 549 ± 18.1 μmol/min, P < 0.01) as showed in Figure 10B. This trend was also apparent, but not statistically significant when mice were water loaded in combination with dDAVP (WT; 499 ± 20.0 μmol/min vs. Epac1$^{-/-}$; 651 ± 73.3 μmol/min, P = 0.10).

When the urea, osmolytes and electrolyte clearances was related to creatinine clearance, estimating the fractional clearance, no significant difference was apparent between water-loaded, nor between water loaded and dDAVP treated WT and Epac1$^{-/-}$ mice (Figure 10D, F, H and J). The same were true when assessing the response to dDAVP in individual animals, by evaluating the altered levels of the substances measured (results not shown). This indicates a normal medullary urea and overall osmolyte reabsorption in Epac1$^{-/-}$ mice.

The fractional Na^+ clearance was significantly reduced by dDAVP in both WT (P < 0.05) and Epac1$^{-/-}$ (P < 0.01), the reduction being most prominent in Epac1$^{-/-}$ mice (Figure 10F). Also the fractional clearance of K^+ was reduced by dDAVP treatment in the Epac1$^{-/-}$ animals (Figure 10H). A minor reduction in fractional urea reabsorption in response to dDAVP could be indicated.

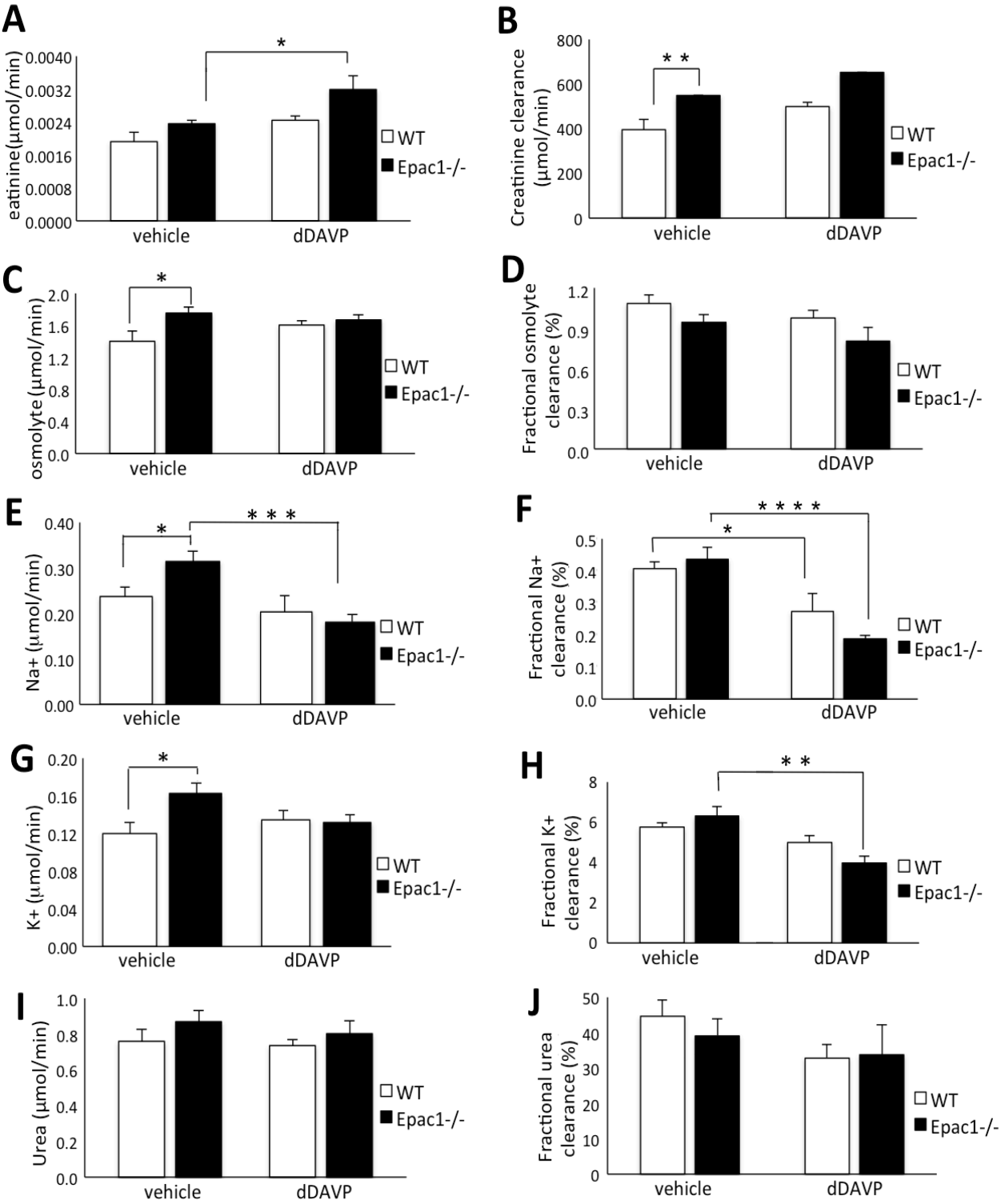

Figure 10: Solute excretion, and fractional clearance, the effect of dDAVP. Urine was collected from individual WT (n = 6) and Epac1$^{-/-}$ mice (n = 6), first receiving water load, and thereafter treated with dDAVP in combination with the water load (collected in 6 h). Plasma samples were collected at termination of the latter experiment. **(A)** and **(B)** Creatinine excretion and clearance of creatinine, both in µmol/min. **(C) - (J)** Excretion and fractional clearance of analyzed substances. Values are presented as means ± SEM, *P < 0.05, **P < 0.01, *** P < 0.001, ****P < 0.0001.

3.2.2 Urinary cAMP in Epac1$^{-/-}$ and WT mice, the effect of dADVP

The differential dDAVP response of the Epac1$^{-/-}$ relative to WT mice raises the question that Epac1$^{-/-}$ mice may have altered AVP signaling. The first step of the renal anti-diuretic effect of AVP is through binding to its V2 receptor, which then stimulates cAMP synthesis. Hence, it was of interest to determine the cAMP level in the urine of Epac1$^{-/-}$ mice. This could give an indication of whether the V2 receptor – cAMP pathway is effective in the Epac1$^{-/-}$ mice. For this the cAMP concentration of individual urine samples was determined by an assay based on competitive displacement of [^{3}H]cAMP by cAMP from binding to site B of the RIα subunit of PKA type I.

The results are displayed in Figure 11, and show a significantly higher cAMP excretion in Epac1$^{-/-}$ mice, relative to urine samples of WT animals. This was true both after water loading (WT; 4.50 ± 0.596 pmol/min vs. Epac1$^{-/-}$; 6.29 ± 0.309 pmol/min, P = 0.02) and following water loading combined with the dDAVP treatment (WT; 8.16 ± 0.481 pmol/min vs. Epac1$^{-/-}$; 11.9 ± 1.26 pmol/min, P = 0.04). Thus the altered Epac1$^{-/-}$ mouse diuresis is unlikely to be due to ineffective V2 receptors, ineffective coupling of V2 to AC, or excessive cAMP degradation. The urine cAMP was significantly increased (P < 0.01) in response to the dDAVP treatment for both Epac1$^{-/-}$ and WT animals.

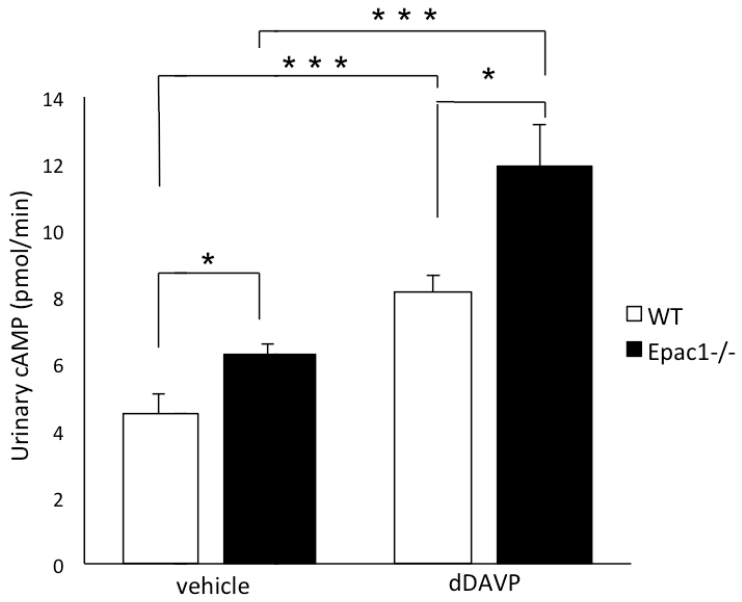

Figure 11: Urine cAMP in Epac1$^{-/-}$ mice. Urine cAMP was determined in samples from WT (n = 6) and Epac1$^{-/-}$ mice (n = 6), collected from the same group of animals, first receiving water load, and thereafter treated with dDAVP in combination with the water load (collected in 6 h). Values are expressed as pmol/min, and are presented as means ± SEM, *P < 0.05, **P < 0.01, ***P < 0.001.

3.2.3 Relative AQP-2 and UT-A1 mRNA and protein expression in Epac1$^{-/-}$ mice

The high cAMP levels in urine from dDAVP treated Epac1$^{-/-}$ mice indicated that they had an intact V2 receptor mediated cAMP increase. We therefore studied whether key downstream cAMP targets mediating the anti-diuresis of AVP could be under-expressed. The expression was investigated both on the gene transcript level, by qRT-PCR, and protein expression level, by immunoblotting. For both analyses WT (n = 4) and Epac1$^{-/-}$ animals (n = 4), receiving water load and euthanized after 3 h later, served as controls (Mce from the second series of mice, see Figure 6B in Methods). They were compared with the WT (n = 6) and Epac1$^{-/-}$ mice (n = 7) that had been water loaded and injected with dDAVP. They were euthanized 6 h (n = 4 WT and n = 5 Epac1$^{-/-}$ mice) or 24 h (n = 2 WT and n = 2 Epac1$^{-/-}$ mice), after the dDAVP administration. The 24 h time point enabled the evaluation of lasting temporal changes in AQP-2 and UT-A1 expression following dDAVP stimulation.

The qRT-PCR analysis, presented in Figure 12A and B, failed to reveal any significant differences in AQP-2 or UT-A1 mRNA level, either in response to dDAVP administration, or between WT and Epac1$^{-/-}$ mice.

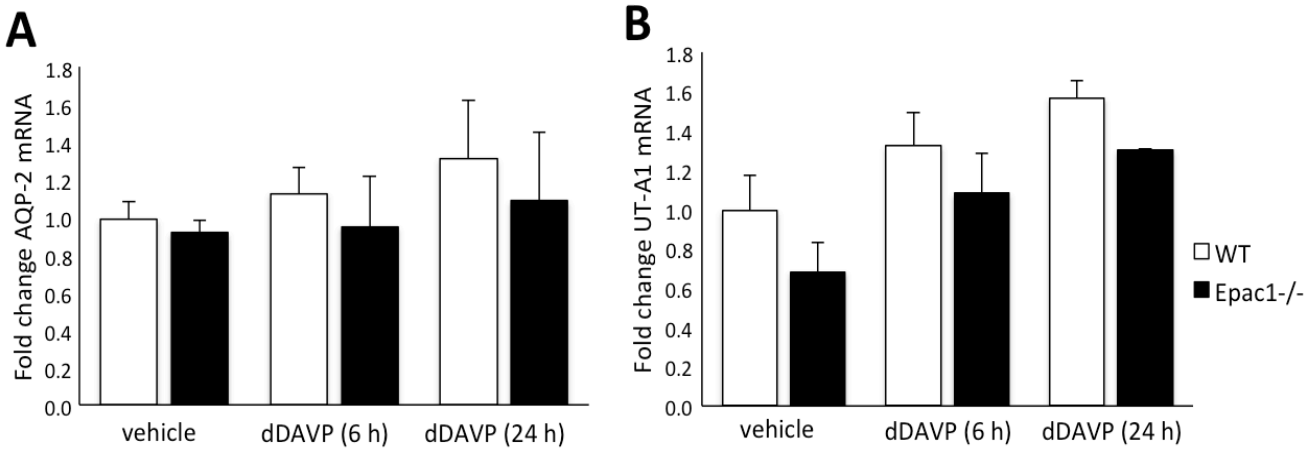

Figure 12: Relative AQP-2 and UT-A1 mRNA levels in Epac1$^{-/-}$ mice total kidney tissue. (A) and **(B)** AQP-2 and UT-A1 mRNA levels were assessed by qRT-PCR in total kidney tissue from a control group of WT (n = 4) and Epac1$^{-/-}$ mice (n = 4), receiving a water load, euthanized after 3 h. They were compared to a second and third group with mice injected with dDAVP before water loaded and euthanized after 6 h (n = 4 WT and n = 5 Epac1$^{-/-}$ mice) and after 24 h (n = 2 for both WT and Epac1$^{-/-}$ mice). AQP-2 and UT-A1 expression were related to expression of the reference genes SDHA, Pkg1, and Ppia. Results are means of three independent determinations. Values are presented as the relative AQP-2 and UT-A1 expression by dividing the means for individual animals by the mean value for water loaded WT littermates. Values are presented as means ± SEM.

The immunoblot experiments demonstrated that the AQP-2 protein existed as two size variants of 29 and 35-55 kDa, corresponding to non-glycosylated (ng) and glycosylated (g) forms (Figure 13A). The densitometric analysis showed no clear difference in AQP-2 protein expression between WT and Epac1$^{-/-}$ mice (Figure 13B). This was true when the g and ng

AQP2 protein bands were evaluated separately (not shown) or jointly. If anything, the Epac1$^{-/-}$ mice had slightly higher AQP-2 protein expression level relative to WT mice 6 h after dDAVP administration. Furthermore, dDAVP appeared to increase the AQP-2 protein expression level in both WT and KO mice.

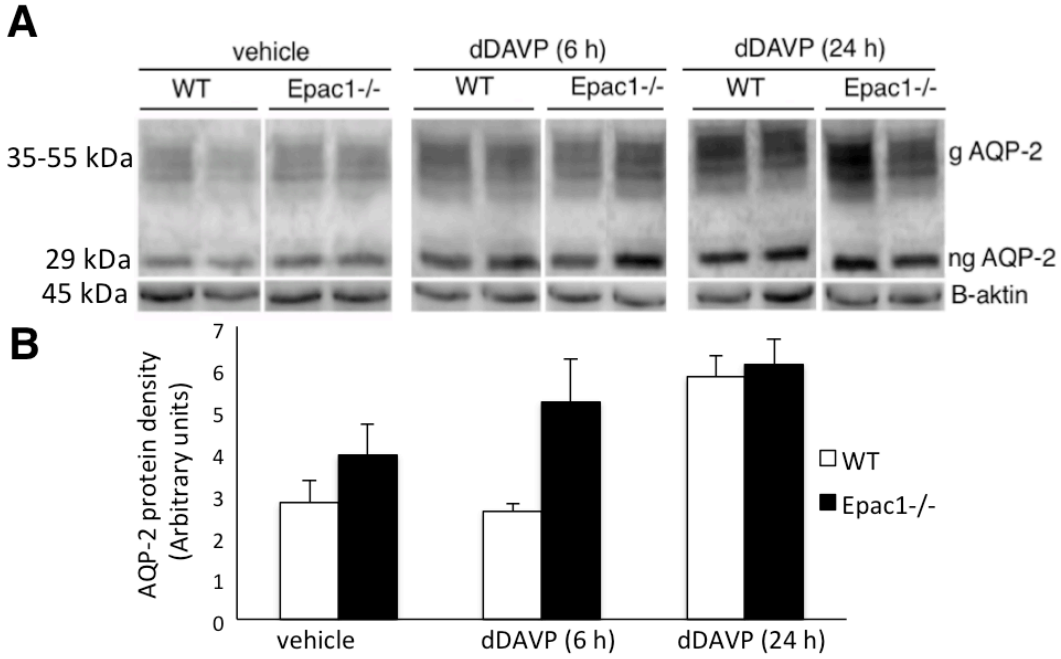

Figure 13: Immunoblots assessing AQP-2 protein abundances in Epac1$^{-/-}$ animals whole kidney homogenates. AQP-2 protein levels determined in a control group of WT (n = 4) and Epac1$^{-/-}$ mice (n = 4), water loaded before euthanized after 3 h. They were compared to a second and third group of mice water loaded in combination with dDAVP administration, before euthanized after 6 h (n = 4 WT and n = 5 Epac1$^{-/-}$ mice) and after 24 h (n = 2 for both WT and Epac1$^{-/-}$ mice). **(A)** Each lane were loaded with 100 µg sample, and probed with an anti AQP-2 antibody. Two bands were detected, a glycosylated (g) and a non-glycosylated (ng) form. AQP2 expression was normalized to β-actin as a loading control. Results from two representative animals from each group are shown. **(B)** Values are mean band densities in arbitrary units (AU) of individual mice, normalized to actin as loading control. Values are presented as means ± SEM.

3.3 Urine albumin in Epac1$^{-/-}$ mice

An increased urine albumin excretion in Epac1$^{-/-}$ mice could reveal if Epac1 is involved in maintaining the selectivity of the GFB. Included in this analysis were urine samples of a selection of the first series of WT (n = 4) and Epac1$^{-/-}$ mice (n = 4). Samples were collected in 6 h after water loading, and subsequently after water loading in combination with dDAVP administration. Urine albumin excretion was related to creatinine (albumin/creatinine ratio) to account for variability in diuresis. No statistical significant difference was observed in albumin/creatinine ratio after water loading (WT; 70.0 µg/mg vs. Epac1$^{-/-}$; 76.4 µg/mg) displayed in Figure 14. The difference was numerically lower in WT relative to Epac1$^{-/-}$

animals after water loading in combination with the dDAVP injection, but still far from statistically significant (WT; 34.0 μg/mg in vs. Epac1$^{-/-}$; 64.9 μg/mg, P = 0.28).

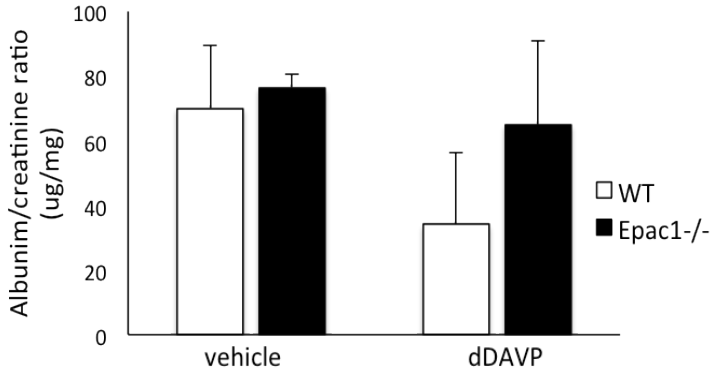

Figure 14. Albuminuria expressed as urine albumin/creatinine ratios in Epac1$^{-/-}$ mice. Urine samples were collected for WT (n = 4) and Epac1$^{-/-}$ mice (n = 4) during 6 h after water loading alone, and after water loading in combination with dDAVP treatment. The urine level of albumin and creatinine was determined. The albumin urine excretion is shown relative to that of creatinine (μg albumin/mg creatinine). Values are presented as means ± SEM.

3.4 The effect of tuboglomerular feedback inhibition by furosemide in Epac1$^{-/-}$ mice

Creatinine clearance is a commonly used method to estimate the glomerular filtration rate (GFR). We found a significant increase of creatinine clearance in water loaded Epac1$^{-/-}$ mice (Figure 10A), indicating GFR to be higher. The loop diuretic furosemide block the TGF control of GFR by inhibiting the NKCC2 of thick ascending loop of Henle and *macula densa*. Furosemide thus can give clues as to whether Epac1 may be involved in the TGF.

The background for the following series of experiments is the proposed increase in GFR in water loaded mice. Also, we wanted to investigate the possibility of Epac 1 involvement in TGF. A second series of mice (See Figure 6B in the method section) were separated in two groups: WT (n = 4) and Epac1$^{-/-}$ mice (n = 4) receiving an oral water load and an i.p. vehicle injection (0.9 % NaCl) and WT (n = 4) and the Epac1$^{-/-}$ mice (n = 4) receiving oral water load and an i.p. furosemide injection (40 μg/g body weight). The animals were further placed in metabolic cages, and urine was continuously collected for 3 h. One of the 4 Epac1$^{-/-}$ mice injected with vehicle in addition to the water load, did not excrete measurable quantities of urine. This was due to technical problems, and consequently, this animal was excluded from the analysis.

When receiving water load and vehicle injection, a minor difference in total urine output between WT and Epac1$^{-/-}$ animals could be observed (P = 0.12) displayed in Figure 15. This was similar to the difference 3 h into the previous water loading experiment from the first series of mice (Figure 7). As expected, furosemide significantly augmented the diuresis during the 3-h period, relative to the mice that received the vehicle injection. WT animals receiving furosemide had a 37.9 % significantly increased total urine output, relative to water loaded vehicle treated WT mice (1.58 ± 0.141 vs. 2.55 ± 0.135 ml, P < 0.01). Epac$^{-/-}$ mice displayed a similar difference of 21.6 % increase, although it was non-significant (2.02 ± 0.172 vs. 2.57 ± 0.174 ml, P = 0.0819). The total urine output in the WT compared to the Epac1$^{-/-}$ mice receiving furosemide injections in addition to the water load showed no difference.

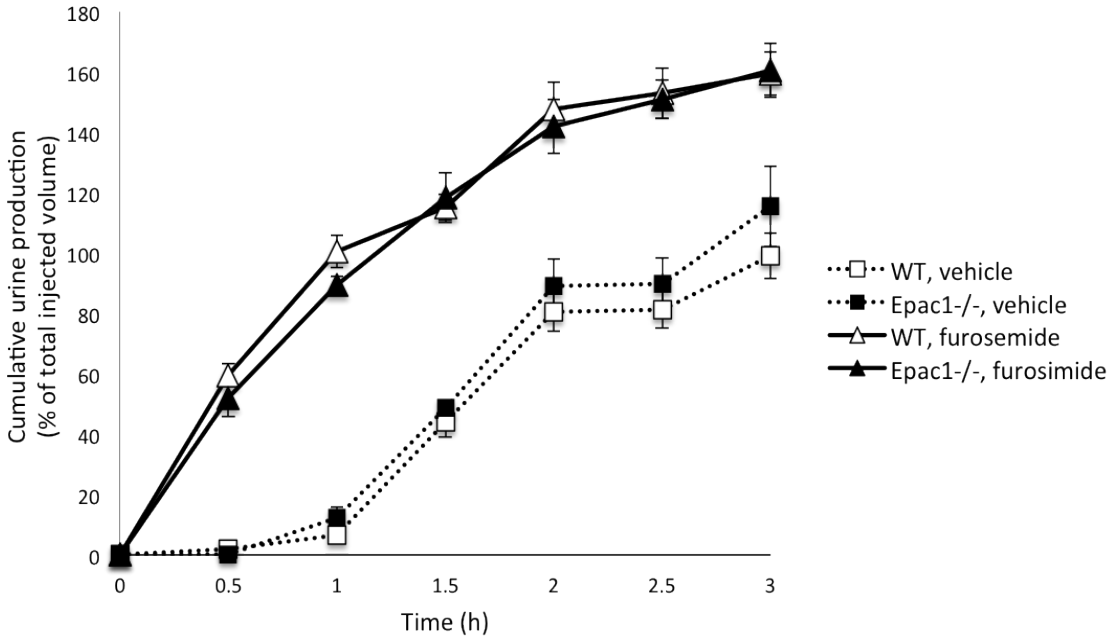

Figure 15: Diuresis after water loading ± furosemide injection. The second series of WT (n = 4) and of Epac1$^{-/-}$ mice (n = 3) received water load, and WT (n = 4) and of Epac1$^{-/-}$ mice (n = 4) received water load and a furosemide injection. Urine were collected in 3 h. Data are presented as cumulative percentage urine excreted of the total injected volume (1.6 ml). Values are presented as means ± SEM.

3.5.1 Solute excretion and fractional clearance in Epac1$^{-/-}$ mice, the effect of furosemide

Urine samples from WT (n = 4) and Epac1$^{-/-}$ mice (n = 3) receiving an oral water load and vehicle injection, and WT (n = 4) and the Epac1$^{-/-}$ mice (n = 4) receiving oral water load and

furosemide injection, together with plasma samples collected after the experiment, were further analyzed.

When evaluating the excretion of creatinine Epac1$^{-/-}$ mice relative to WT animals, no significant differences were detected (Figure 18A). A trend was that water loaded Epac1$^{-/-}$ mice had a higher creatinine excretion level, relative to WT. In furosemide treated mice the trend were opposite. The creatinine clearance, and thus the GFR, were higher in water loaded Epac1$^{-/-}$ relative to WT mice, consistent with what was found in the water loading of the first series of mice (Figure 16 B and Figure 10B, respectively). In the furosemide treated mice the observed increase in GFR of Epac1$^{-/-}$ mice was abolished, with creatinine clearance values 553 ± 121.9 µl/min in WT and 606 ± 64.01 µl/min in Epac1$^{-/-}$.

As displayed in Figure 16C and D, the excreted osmolytes, and the fractional osmolyte clearance were significantly higher in furosemide treated mice. Accompanying the increase in osmolyte excretion, following the furosemide injection was a significantly higher excretion and fractional clearance of Na^+ and K^+ (K^+ excretion was only statistically significant in the WT mice), displayed in Figure 16E to H. This reflects inhibition of NaCl reabsorption in the thick ascending loop of Henle.

Figure 16I and J present the urea excretion. Furosemide caused urea excretion in Epac1$^{-/-}$ animals to be significantly decreased ($P = 0.01$). Furthermore, the fractional urea clearance showed a significant decrease in urea excretion in Epac1$^{-/-}$, relative to WT mice ($P = 0.03$).

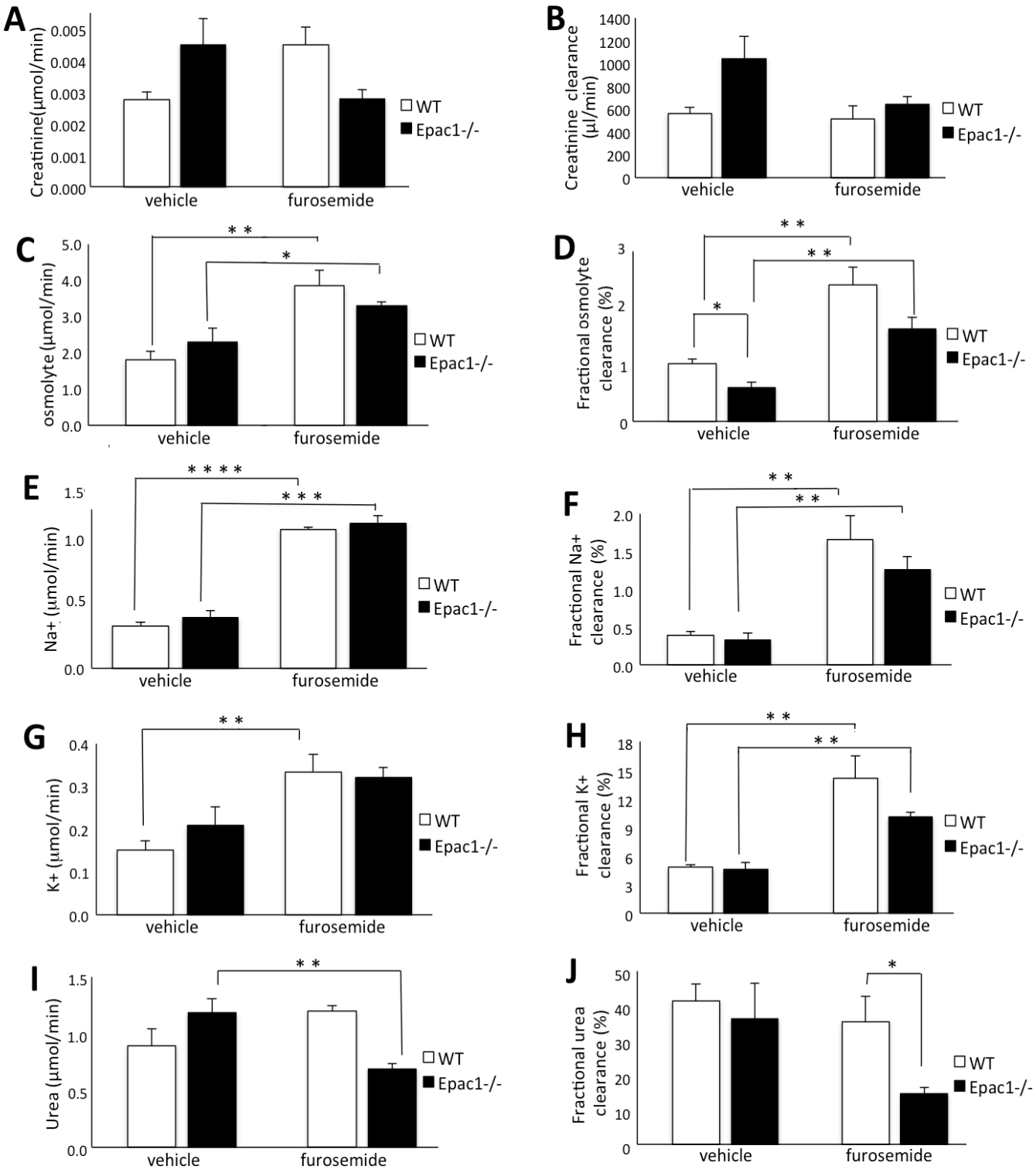

Figure 16: Excretion, and fractional solute clearance, the effect of furosemide. Urine samples were collected from second series of WT (n = 4) and Epac1$^{-/-}$ mice (n = 3) receiving water load and a vehicle injection, and WT (n = 4) and Epac1$^{-/-}$ mice (n = 4) receiving water load a furosemide injection. The urine was collected for 3 h. Plasma samples were collected after the experiment. **(A)** and **(B)** Creatinine excretion and clearance of creatinine, both in µmol/min. **(C) - (J)** Excretion and fractional clearance of analyzed urine constituents. Values are presented as means ± SEM, *P < 0.05, **P < 0.01, *** P < 0.001, ****P < 0.0001.

Urine cAMP was determined from individual mice frond second series. No significant differences were observed either in response to furosemide, nor between WT and Epac1$^{-/-}$ animals, displayed in Figure 17.

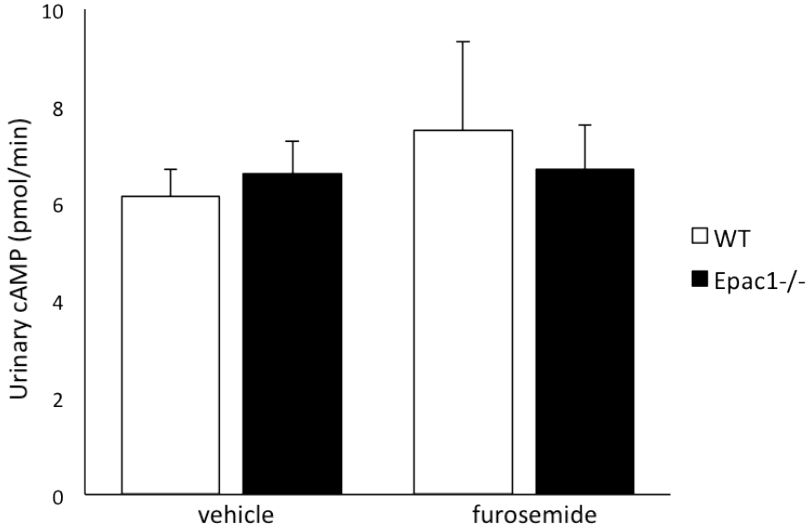

Figure 17: Urine cAMP in Epac1$^{-/-}$ mice. Urine cAMP was determined in urine samples from the second series of WT (n = 4) and Epac1$^{-/-}$ mice (n = 3) received water load and vehivle treatment, and WT (n = 4) and Epac1$^{-/-}$ mice (n = 4) received water load and a furosemide injection. The urine was collected for 3 h. Values are expressed as pmol/min, and are presented as means ± SEM.

4 Discussion

The kidney is one of the organs with highest expression levels of Epac1 (12, 13). The present study uses an animal model constructed in our research group, where Epac1 has been knocked out. This enables us to study the Epac1 function *in vivo*. Furthermore, such Epac1$^{-/-}$ animals can tell whether previous *in vitro* studies implicating Epac1 in regulation of renal channels and transporters (65, 68-73), and in regulation of the GFB (75) are relevant under *in vivo* conditions.

We demonstrate here that the Epac1$^{-/-}$ mice have a modest polyuria relative to their WT littermates, during baseline conditions. To explore the nature of the polyuria, mice were investigated after oral water load, with and without dDAVP administration. Under these conditions we measured renal excretion and/or fractional clearance of osmolytes, electrolytes, urea, creatinine, cAMP, and albumin. We conclude that Epac1$^{-/-}$ mice have a preserved ability dilute and concentrate urine, however a slightly deficient urine concentrating ability in response to vasopressin was detected. They have also a heightened glomerular filtration rate, presumably due to less efficient tubulo-glomerular feedback. The findings in the current study and conclusions are discussed in more detail below.

4.1 Epac1$^{-/-}$ mice have increased diuresis

This study confirmed the notion of a modest polyuria of the Epac1$^{-/-}$ animals observed in preliminary experiments in our group (unpublished observations). At baseline Epac1$^{-/-}$ mice revealed a 2.4 fold increase in diuresis relative to their WT littermates, whose diuresis agreed with that observed in other studies (84). The polyuria of the Epac1$^{-/-}$ mice was accompanied by a 2.2 fold increase in water consumption and a 1.5 fold decreased in urinary osmolality, although these differences were not statistically significant (Table 1). The excretion of Na^+, K^+, urea and creatinine were not different (Table 1). Collectively, these data suggests that the Epac1$^{-/-}$ mice are water diuretic, e.g. consumes and excretes more water than WT mice.

In all previous experiments mice have had free access to water (and food). It can be argued that the increased diuresis observed in the Epac1$^{-/-}$ mice has its origin in an altered drinking behavior. Additionally it is possible that leakage from the water bottles, and evaporation from the urine collection tubes affected the results to some extent. To determine the nature of the

increased diuresis, and to strengthen the hypothesis of polyuria, new experiments were designed. More comparable states of hydration between the animals was achieved by water deprive animals 1 h prior to the experiment, and empty urine bladders by bladder massage, before introduce an oral water load. Urine collected in the following 6 h demonstrated that Epac1$^{-/-}$ mice excreted a significantly higher total urine volume, relative to WT mice (Figure 7). These results demonstrate that the polydipsia conceivably is not the primary cause of the modest polyuria in the Epac1$^{-/-}$ mice.

Water loading suppresses endogenous vasopressin in the animals (41), and thus enables evaluation of their ability to dilute the urine. Epac has been implicated in down-regulation of the NHE3 in the proximal tubule and thick ascending limb of Henle (68, 69), and in activating the ion-pump H^+-K^+-ATPase along the collecting duct (65). Along the apical membrane of collecting duct elevated cAMP levels promote trafficking and insertion of epithelial sodium channels (ENaC), responsible for Na^+ reabsorption (85). This stimulation is proposed to involve Epac in lung cells (86), but may also apply to collecting duct cells. It could be suggested that altered activation of these transporters could cause Epac1$^{-/-}$ mice to have a reduced urine diluting capacity, hence, less tubular reabsorption and increased amount of electrolytes excreted in the urine. On the contrary, the fractional clearance of total osmolytes, Na^+ and K^+ was similar in Epac1$^{-/-}$ relative to WT mice (Figure 10D, F, and H). Moreover the present study demonstrated, that the urinary osmolality during water loading was low in both Epac1$^{-/-}$ (233 mOsmol/kgH_2O) and WT mice (249 mOsmol/kgH_2O) and not significantly different ($P = 0.3$) (Figure 9A). Based on these observations it can be concluded that Epac1$^{-/-}$ mice are capable of diluting urine, and to excrete water and salt independently to the same extent as their WT littermates. It should be noted that plasma Na^+ or K^+ used to calculate fractional excretion were taken from the literature, as their levels are relatively constant (87).

These results do not exclude the possibility of Epac1 being involved in regulation of the NHE3 and the H^+-K^+-ATPase, or possibly ENaC, as the deletion of Epac1 could be compensated for. Other renal channels and transporters would possibly increase their activity in the Epac1$^{-/-}$ animals. Moreover are the channels postulated to be regulated by Epac, also regulated by PKA (65, 68-73), the second major cAMP receptor. Thus, it could be postulated that PKA might constitute a compensatory mechanism, enabling Epac1$^{-/-}$ mice to maintain its

renal functions. These results can nevertheless propose that Epac role in regulation of NHE3 and H^+-K^+-ATPase is not relevant under *in vivo* conditions.

4.2 Epac1$^{-/-}$ mice have subtly deficient response to vasopressin

Having recognized Epac1$^{-/-}$ mice intact urine diluting ability, and a possible water diuresis, the effect of the anti-diuretic hormone vasopressin (AVP) was investigated to evaluate the urine concentrating capacity. Binding of AVP to its V2 receptor, lead to increase cAMP production and subsequent induction of anti-diuresis (45). Epac has been proposed a role in activating the AVP regulated water channel AQP-2 in distal tubule and collecting duct, and urea transporter UT-A1 regulated by AVP in the inner medullary collecting duct (70-74).

Water loading experiments and a subsequent dDAVP injection resulted in a vast reduction in urine flow relative to when mice were water loaded (Figure 8). This was true for WT and Epac1$^{-/-}$ mice, settling that Epac1$^{-/-}$ mice do not have any major perturbations in dDAVP response. Urine osmolality is a key parameter in determination of the dDAVP effect. dDAVP increased the urine osmolality significantly in Epac1$^{-/-}$ mice, however not to the same extent as in the WT littermates. The results revealed that the percentage increased osmolality in individual animal urine samples was significantly attenuated in the Epac1$^{-/-}$ mice with a 77 % increase, relative to the WT mice presenting a mean increase of 163 % ($P = 0.02$, see Figure 9B). The same were illustrated with the renal free water clearance, which was significantly higher (less negative) in Epac1$^{-/-}$ mice following the dDAVP administration compared to WT mice (Figure 9D). These results propose that deletion of Epac1 causes mice to have significantly reduced water-retaining capacity in response to dDAVP.

It is interesting to note that when the mice were only water loaded, a difference between Epac1$^{-/-}$ and WT mice were not observed until excretion of 100 % of introduced water was completed, i.e. 1 to 1.5 h after oral water load (Figure 7). Thus, the increased water loss in Epac1$^{-/-}$ relative to WT mice must have occurred during increasing endogenous AVP levels in agreement with the observation of an attenuated response to dDAVP (Figure 9B).

Acute water loading and dDAVP treatment will have opposing effects, as the animals will when water loaded try to excrete access water and down regulate endogenous AVP levels, while the dDAVP injection will force the animal to retain the water and concentrate the urine.

Despite this the dDAVP treatment seemed to have a proper effect. dDAVP tended to decrease the fractional Na^+ and K^+ clearance in both WT and Epac1$^{-/-}$ mice (Figure 12F and H). This is in agreement with the effects of AVP along the renal tubule on Na^+ (88) and K^+ transport (89), and what is shown *in vivo* at the concentrations used in the current study (90, 91). Also the fractional urea clearance was somewhat reduced (Figure 12J), corroborating with dDAVP-induced urea reabsorption via activation of UT-A1 (59).

The first step of the renal anti-diuretic effect of AVP is through binding to its V2 receptor, which subsequently stimulates cAMP synthesis (45). Thus as cAMP is a mediator of AVP effects the cAMP level in the urine of Epac1$^{-/-}$ mice could give an indication of whether the V2 receptor – cAMP pathway is effective in the Epac1$^{-/-}$ mice. Cyclic AMP is excreted from the kidney into the urine (92, 93). The source is partly cAMP filtrated from plasma by glomerular filtration, and partly endogenous cAMP derived from renal cells and transported across the apical membrane of tubule cells inn to the renal tubules, via an energy dependent putative efflux pump (94, 95). There are conflicting results on the relative amounts. It has been found that about three quarter of the cAMP excreted arises from filtrated plasma, and the remaining quarter is derived from renal cells (95, 96). However others have showed that most of the urinary cAMP is derived from renal cells, and that urinary cAMP generally reflects proximal tubule parathyroid hormone-mediated AC activity (97). These contradicting results are due to the difficulties in determining endogenous cAMP. In the present study the blood plasma from each mouse was analyzed for several parameters and the amount left was insufficient to determine the low plasma cAMP level.

Urinary cAMP levels however revealed to be significantly increased in response to dDAVP treatment. These findings are consistent with the effect of hormones that stimulate renal AC, such as AVP and PTH, which have been reported to increase cAMP excretion (95). Water loading, which will suppress AVP secretion, has been shown to depress urinary cAMP (98), and notably could bias the results. Epac1$^{-/-}$ mice showed, relative to WT animals, a significant increase in urinary cAMP (Figure 11). This was true both after water loading and following water loading combined with dDAVP administration. Thus the reduced response to dDAVP in the Epac1$^{-/-}$ mice is not likely due to a reduced sensitivity of the V2 receptor, or to increased cAMP degradation. Rather, the phenotypes observed are more probably due to deficient response to cAMP, as expected for deletion of the cAMP effector Epac1.

In an anti-diuretic state induced by dDAVP, urea reabsorption in the renal medulla is enhanced to prevent an osmotic diuretic effect of urea and thereby achieve the high urine concentration capacity (59). Epac has as mentioned, been suggested to be involved in the regulation of UT-A1 trafficking to the apical membrane of inner medulla collecting duct cells (73, 74). A perturbation in medullary vasopressin induced urea reabsorption could explain Epac1$^{-/-}$ mice slightly reduced ability to conserve water in response to vasopressin. This is clearly demonstrated in UT-A1/3$^{-/-}$ animals showing a urea-induced diuresis (99). Epac1$^{-/-}$ mice did however not show an altered fractional urea clearance, relative to WT mice, in response to the dDAVP treatment (Figure 10J). The same was true when using each mouse as its own control, evaluating the individual mice reduced fractional urea clearance when water loaded relative to when dDAVP treated. WT and Epac1$^{-/-}$ mice had a similar reduction of 26 % and 23 %, respectively. These results was supported by qRT-PCR analyzes of UT-A1 mRNA expression level, which was not altered in the Epac1$^{-/-}$ mice (Figure 12B). Two antibodies tested for UT-A1 failed to detect the proteins. This proposes that deletion of Epac1 does not affect the urea reabsorption relative to WT littermates. Thus in vivo it is evidence for renal urea handling not being different when Epac1 is deleted. Epac1 role in UT-A1 trafficking can however not be excluded, as PKA possibly could compensate for the deletion of Epac1.

The indications of water diuresis in Epac1$^{-/-}$ mice, together with the attenuated response to dDAVP, and no sign of urea-induced diuresis, suggests reduced water reabsorption through the AVP regulated AQP-2. A collecting duct AQP-2$^{-/-}$ mice model demonstrated a 10-fold increased urine production (100). AQP-2 regulation involving Epac1 is in agreement with several *in vitro* studies (70-72). No gross differences were however observed between WT and Epac1$^{-/-}$ mice on AQP-2 mRNA expression level (Figure 12A). The same was true for the AQP-2 protein level (Figure 13A and B). It can be proposed that Epac1$^{-/-}$ mice had a slightly higher AQP-2 protein level relative to WT animals, most prominent 6 h after water load and dDAVP treatment. This proposed trend contradicts with the reduced urine concentrating abilities observed in the Epac1$^{-/-}$ mice, and with *in vitro* studies implicating Epac in the AQP-2 up-regulation.

It must be noted that it was the total AQP-2 protein abundance that was investigated. No conclusion can be made about the localization of the AQP-2 proteins. They could be both active localized in the apical membrane, or in intracellular vesicles. As there is indications of reduced water reabsorption, and attenuated response to AVP in the Epac1$^{-/-}$ mice it can be

speculated that Epac1 most prominent role in regulation of AQP-2 is in vesicle trafficking to the apical membrane, together with PKA (Figure 18). Hence, the Epac1$^{-/-}$ mice would have a reduced level of apical membrane AQP-2 contributing in water reabsorption, although the total level is the same as in the WT littermates. Further analysis should involve analysis of subcellular localization, either by using antibodies for the phosphorylation states of AQP-2 or by immunohistochemistry.

We hypothesize that the possible minor increase in total AQP-2 protein expression, is due to an alternative AQP-2 up-regulation mechanism. It could act to compensate for the decrease in water reabsorption in the Epac1$^{-/-}$ animals. This could cause synthesis or reduced proteosomal degradation of the water channel. The analyses of both mRNA and protein expression showed a weak effect of dDAVP, relative to the water loaded control mice. This was coherent with, the modest dose given, and vasopressin's role in the transcription of these proteins (57, 63, 64).

Restricted access to animals and tissue caused lack of measurements of the basal AQP2 and UT-A1 mRNA and protein expression level. All mice were water loaded, which conceivably is a confounding factor in the analysis. Most studies demonstrate that AQP-2 and UT-A1 mRNA in mice kidney, is relatively constant after water loading (84, 101), hence it can be suggested that water loading not affected the mRNA analyses to a great extent. Water loading has however demonstrated to down regulate AQP-2 protein (51, 84), and it has been implicated that regulation of the degradation of renal AQP-2 protein as a urine diluting mechanism during acute water loading (84). It thus conceivable that AQP-2 level in this study is down regulated. Moreover the down-regulation mechanism could be different in the Epac1$^{-/-}$ mice relative to WT animals. For further analyses mice not receiving water loading should thus be included as controls.

4.3 Increased glomerular filtration rate in Epac1$^{-/-}$ mice

Glomerular filtration rate (GFR) is determined by filtration pressure together with the hydraulic conductivity and the filtering surface of the capillaries. GFR is kept relatively constant despite changes in systemic blood pressure, a phenomenon called auto regulation. An important component of this auto regulation is tubulo-glomerular feedback (TGF) involving the juxtamedullary apparatus (39).

Creatinine clearance studies are frequently used in renal physiology to measure GFR (102). It must be considered that, while the majority of creatinine is excreted into the urine by glomerular filtration, the renal tubules also secrete a finite amount of creatinine (103). Other more accurate markers have been developed, but require intravenous administration (102). Such methods were not feasible in the present study, and the measurement of an endogenous compound, such as creatinine, was more desirable. The creatinine concentration in plasma samples was difficult to determine since the levels in mice were just above the sensitivity of the method with the amount plasma available (10 μl). Thus creatinine clearance was determined by using the mean values of plasma from the first series of the WT (n = 6) and Epac1$^{-/-}$ mice (n = 7) after the experiment with water-loading the dDAVP treatment. The GFR estimates hence, should be considered with this in mind. The plasma values are low relative to the literature values found in mice (104). It is however interesting to note that the creatinine concentration in plasma of Epac1$^{-/-}$ mice were slightly lower, relative to WT animals. This is an indirect indication of a higher GFR.

Water loaded Epac1$^{-/-}$ mice, revealed to have significantly increased GFR relative to the WT littermates (Figure 10B). The increase was supported by a significantly elevated urine excretion of osmolytes, Na^+ and K^+, and cAMP in the Epac1$^{-/-}$ mice, relative to WT animals (Figure 10C, E, G, and Figure 13, respectively). Urea and creatinine showed the same trend although not statistically significant (Figure 10A and I, respectively). An increased GFR would be a conceivable explanation for the higher excretion of the evaluated substances. dDAVP did not increase GFR in the Epac1$^{-/-}$ mice significantly. This corroborates with a similar urine excretion of osmolytes, Na^+ and K^+, urea, and creatinine following water load combined with dDAVP administration.

Several possibilities exist to explain the increased GFR in the Epac1$^{-/-}$ mice. The most obvious explanation is an elevated filtration pressure rather than an increased hydraulic conductivity or filtering surface over the glomerular capillaries (36). Although Epac has been reported to strengthen the vascular endothelial barrier function (105, 106), the renal glomerular filtration barrier (GFB) is different from the inter-endothelial junction, and the outcome of Epac1 deletion is therefore unknown. The explanation that the glomerular filtration barrier is more conductive to water and solutes in the Epac1$^{-/-}$ animals is less

probable, since the GFB generally has a unique ability to filtrate extremely large amounts of solutes, while staying selective to amongst other proteins (36). There is evidence that overstimulation of mesangial cells by angiotensin-II can increase collagen synthesis via Epac1 (75), possibly linked to sclerotic changes and decreased GFR with albuminuria (75, 107). The Epac1$^{-/-}$ animals revealed to have an increased GFR (Figure 10B), and lack of albuminuria (Figure 12), collectively being indicative of an intact filtration barrier.

Increased GFR in the Epac1$^{-/-}$ animals indicates an elevated filtration pressure, if the hydraulic conductivity and the filtering surface of the capillaries are unchanged (36). TGF is an important mechanism of filtration pressure control (38). Changes of tubular NaCl are sensed at the *macula densa*, via NKCC2, and are maily linked to the control of arteriolar resistance (108). TGF is easily studied *in vivo*, by administrating the loop diuretic furosemide. Furosemide inhibits the NKCC2, and thus blocks the TGF (108). A possible defect in the *macula densa* feedback to control of afferent arteriolar tonus could explain the observed increase in GFR during water loading.

The effect of the furosemide administration was evident in both WT and Epac1$^{-/-}$ mice, judging by a highly significant increase of Na^+ (Figure 16E), and K^+ excretion (Figure 16G) (109, 110). The magnitude of the observed furosemide effect was consistent with previous studies in mice using the same dose and administration route (111).

Furosemide appeared to obliterate the difference in GFR between WT and Epac1$^{-/-}$ animals, observed in the water loaded control animals (Figure 16B). The elevated urine excretion of creatinine, osmolytes, Na^+, K^+ and urea observed in water loaded Epac1$^{-/-}$ mice were not apparent for furosemide treated animals, as they were for the water-loaded mice (Figure 16A, C, E and G). We therefor hypothesize that a possibly impaired TGF apparent when Epac1 is deleted can cause the difference in GFR between the WT and Epac1$^{-/-}$ mice. It must be noted that few mice were included in the analysis and we can only speculate. Thus more mice should be included in further experiments.

The NKCC2, responsible for the TGF, is regulated by AVP. Binding of AVP to the V2 receptor, lead to generation of cAMP, which subsequently activates NKCC2 by trafficking to the apical membrane of macula dens and thick ascending limb of loop of Henle (112, 113). Epac1 could be involved in trafficking of NKCC2 as suggested for other transporters and

channels ((65, 68, 70, 73) reviewed in (30)). A study done by Greger et al., of cAMP-induced NKCC2 exocytosis implicated PKA rather than Epac as mediator (107). It should be kept in mind that it relied on the nonspecific PKA inhibitor H-89 (26), and unusually high concentration (1mM) of the PKA activator N^6-Bz-cAMP, which can inhibit PDE's and thereby increase cAMP (21) and thereby activate Epac. Besides, the blocking by H-89 was incomplete (107). Despite the findings by Greger et al., it can be speculated that Epac1 collaborates with PKA to achieve optimal NKCC2 exocytosis in cells of the thick ascending limb of Henle and *macula densa* (Figure 18).

The Epac1$^{-/-}$ mice tended to have lower fractional clearance of osmolytes, Na^+, and K^+ less cAMP excretion than their WT littermates. This could possibly be an indication of that the effects of furosemide were attenuated in Epac1$^{-/-}$ animals, consistent with the hypnotized diminished TGF in these animals. A statistically significant reduction in fractional urea clearance was observed following furosemide treatment. A possible explanation for this has not been addressed in the current study.

In conclusion, Epac1$^{-/-}$ animals exhibit a moderate water diuretic phenotype. The increased urinary flow rate in Epac1$^{-/-}$ mice was associated with a decreased urine osmolality and an increased free water clearance during water conservation, proposing a reduced response antidiuretic hormone vasopressin. The present study shows that the subdued response could possibly not be explained by under-expression of either the AVP-stimulated urea transporter UT-A1 or the water channel AQP-2. A remaining possibility is that Epac1 is required for optimal trafficking of AQP-2 to the apical membrane. Despite the deletion of Epac1, mice were perfectly able to dilute their urine in response to an oral water load. It can therefor be concluded that the cortico-medullary osmotic gradient is intact in the Epac1$^{-/-}$ animals. We finally suggest that Epac1 is involved in tubulo-glomerular-feedback signaling resulting in an increased GFR in Epac1$^{-/-}$mice following water loading possibly via regulating the NKCC2.

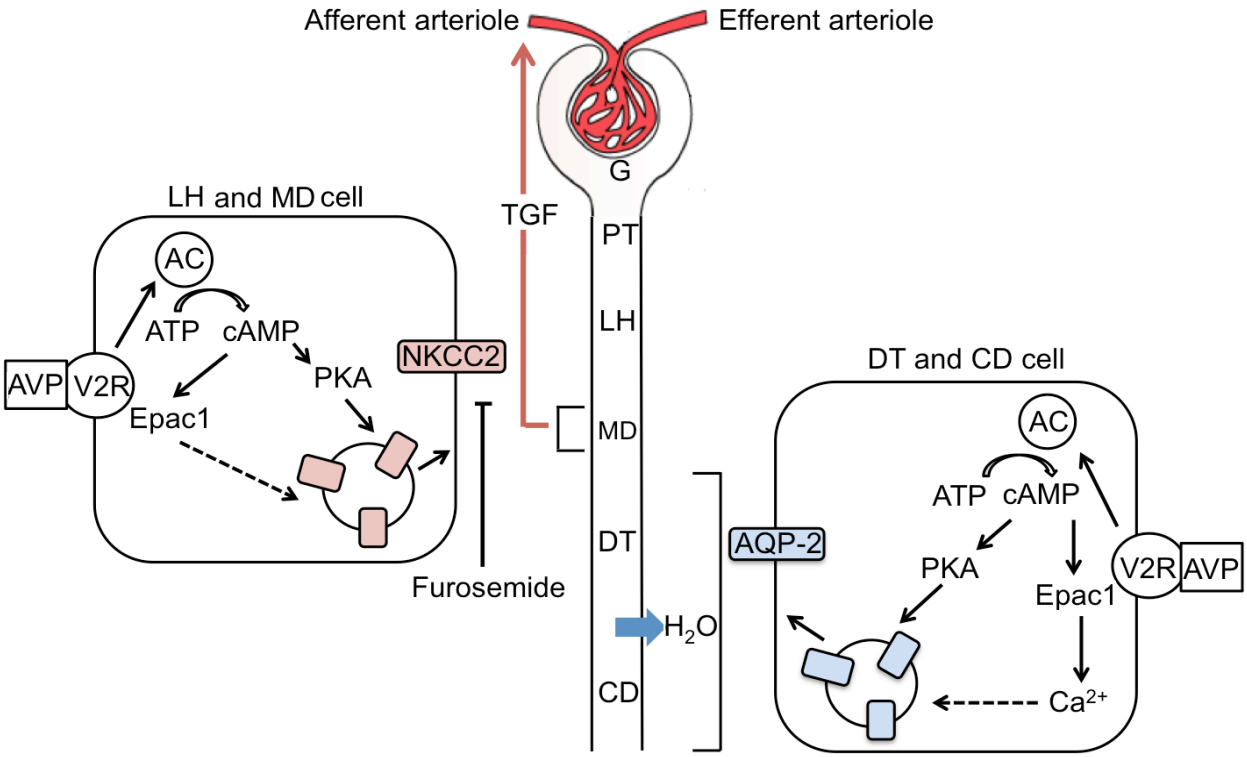

Figure 18: A model for possible roles of Epac1 *in vivo*. Here a schematic nephron is presented, including the glomerulus (G) with afferent arteriole, the glomerular capillaries, and efferent arteriole. The glomerulus is followed by proximal tubule (PT), the loop of Henle (LH), *macula densa* (MD), distal tubule (DT) and finally collecting duct (CD). AVP binding to V2R activate AC and generate cAMP. This subsequently leads to activation of PKA and Epac (45). PKA phosphorylation induces exocytosis of vesicles, containing AQP-2 (54, 55) and NKCC2 (112, 113). Additionally Epac has been implicated in exocytosis of AQP-2 via increase cytosolic Ca^{2+} (56). **(LH and MD cell)** NKCC2 co transporters localized in MD (and LH) is involved in tubulo-glomerular feedback (TGF), mainly by altering resistance in afferent arteriole (red arrow) (39). The observed increase in GFR in Epac1$^{-/-}$ mice was abolished when blocking NKCC2, and thus TGF with furosemide. It can be hypothesized that an impaired TGF were the origin of the increased GFR in Epac1$^{-/-}$, and that the cAMP induced NKCC2 exocytosis possibly involves Epac1 (dashed arrow). **(DT and CD cell)** AQP-2 in localized in DT and CD, and transport water out (blue arrow) (39). A reduced response to dDAVP in the Epac1$^{-/-}$ mice was observed, together with indications of water diuresis, and no sign of urea induced diuresis. Thus, a reduced water reabsorption via AVP regulated AQP-2 could explain this reduced response, and increased amount of excreted water. It can be hypostasized that Epac1 has role in exocytosis of AQP-2 (dashed arrow), as supported by *in vitro* findings (56).

5. References

1. Beavo JA, Brunton LL. Cyclic nucleotide research -- still expanding after half a century. Nature reviews Molecular cell biology. 2002;3(9):710-8.
2. Sunahara RK, Taussig R. Isoforms of mammalian adenylyl cyclase: multiplicities of signaling. Molecular interventions. 2002;2(3):168-84.
3. Nikolaev VO, Gambaryan S, Engelhardt S, Walter U, Lohse MJ. Real-time monitoring of the PDE2 activity of live cells: hormone-stimulated cAMP hydrolysis is faster than hormone-stimulated cAMP synthesis. The Journal of biological chemistry. 2005;280(3):1716-9.
4. Conti M, Beavo J. Biochemistry and physiology of cyclic nucleotide phosphodiesterases: essential components in cyclic nucleotide signaling. Annual review of biochemistry. 2007;76:481-511.
5. Beavo JA, Hardman JG, Sutherland EW. Stimulation of adenosine 3',5'-monophosphate hydrolysis by guanosine 3',5'-monophosphate. The Journal of biological chemistry. 1971;246(12):3841-6.
6. Jensen BO, Selheim F, Doskeland SO, Gear AR, Holmsen H. Protein kinase A mediates inhibition of the thrombin-induced platelet shape change by nitric oxide. Blood. 2004;104(9):2775-82.
7. Beavo JA. Cyclic nucleotide phosphodiesterases: functional implications of multiple isoforms. Physiological reviews. 1995;75(4):725-48.
8. Walsh DA, Perkins JP, Krebs EG. An adenosine 3',5'-monophosphate-dependant protein kinase from rabbit skeletal muscle. The Journal of biological chemistry. 1968;243(13):3763-5.
9. Michel JJ, Scott JD. AKAP mediated signal transduction. Annual review of pharmacology and toxicology. 2002;42:235-57.
10. Podda MV, Grassi C. New perspectives in cyclic nucleotide-mediated functions in the CNS: the emerging role of cyclic nucleotide-gated (CNG) channels. Pflugers Archiv : European journal of physiology. 2013.
11. Schmidt M, Dekker FJ, Maarsingh H. Exchange protein directly activated by cAMP (epac): a multidomain cAMP mediator in the regulation of diverse biological functions. Pharmacological reviews. 2013;65(2):670-709.
12. de Rooij J, Zwartkruis FJT, Verheijen MHG, Cool RH, Nijman SMB, Wittinghofer A, et al. Epac is a Rap1 guanine-nucleotide-exchange factor directly activated by cyclic AMP. Nature. 1998;396(6710):474-7.
13. Kawasaki H, Springett GM, Mochizuki N, Toki S, Nakaya M, Matsuda M, et al. A family of cAMP-binding proteins that directly activate Rap1. Science. 1998;282(5397):2275-9.
14. de Rooij J, Rehmann H, van Triest M, Cool RH, Wittinghofer A, Bos JL. Mechanism of regulation of the Epac family of cAMP-dependent RapGEFs. The Journal of biological chemistry. 2000;275(27):20829-36.
15. Rehmann H, Arias-Palomo E, Hadders MA, Schwede F, Llorca O, Bos JL. Structure of Epac2 in complex with a cyclic AMP analogue and RAP1B. Nature. 2008;455(7209):124-7.
16. Rehmann H, Prakash B, Wolf E, Rueppel A, de Rooij J, Bos JL, et al. Structure and regulation of the cAMP-binding domains of Epac2. Nature structural biology. 2003;10(1):26-32.

17. Ponsioen B, Gloerich M, Ritsma L, Rehmann H, Bos JL, Jalink K. Direct spatial control of Epac1 by cyclic AMP. Molecular and cellular biology. 2009;29(10):2521-31.
18. Rehmann H, Das J, Knipscheer P, Wittinghofer A, Bos JL. Structure of the cyclic-AMP-responsive exchange factor Epac2 in its auto-inhibited state. Nature. 2006;439(7076):625-8.
19. Gloerich M, Bos JL. Epac: defining a new mechanism for cAMP action. Annual review of pharmacology and toxicology. 2010;50:355-75.
20. Christensen AE, Selheim F, de Rooij J, Dremier S, Schwede F, Dao KK, et al. cAMP analog mapping of Epac1 and cAMP kinase. Discriminating analogs demonstrate that Epac and cAMP kinase act synergistically to promote PC-12 cell neurite extension. The Journal of biological chemistry. 2003;278(37):35394-402.
21. Poppe H, Rybalkin SD, Rehmann H, Hinds TR, Tang XB, Christensen AE, et al. Cyclic nucleotide analogs as probes of signaling pathways. Nature methods. 2008;5(4):277-8.
22. Herfindal L, Krakstad C, Myhren L, Hagland H, Kopperud R, Teigen K, et al. Introduction of Aromatic Ring-Containing Substituents in Cyclic Nucleotides Is Associated with Inhibition of Toxin Uptake by the Hepatocyte Transporters OATP 1B1 and 1B3. PloS one. 2014;9(4):e94926.
23. Herfindal L, Nygaard G, Kopperud R, Krakstad C, Doskeland SO, Selheim F. Off-target effect of the Epac agonist 8-pCPT-2'-O-Me-cAMP on P2Y12 receptors in blood platelets. Biochemical and biophysical research communications. 2013;437(4):603-8.
24. Rehmann H. Epac-inhibitors: facts and artefacts. Scientific reports. 2013;3:3032.
25. Kooistra MR, Corada M, Dejana E, Bos JL. Epac1 regulates integrity of endothelial cell junctions through VE-cadherin. FEBS letters. 2005;579(22):4966-72.
26. Petersen RK, Madsen L, Pedersen LM, Hallenborg P, Hagland H, Viste K, et al. Cyclic AMP (cAMP)-mediated stimulation of adipocyte differentiation requires the synergistic action of Epac- and cAMP-dependent protein kinase-dependent processes. Molecular and cellular biology. 2008;28(11):3804-16.
27. Cheng X, Ji Z, Tsalkova T, Mei F. Epac and PKA: a tale of two intracellular cAMP receptors. Acta biochimica et biophysica Sinica. 2008;40(7):651-62.
28. Dodge-Kafka KL, Soughayer J, Pare GC, Carlisle Michel JJ, Langeberg LK, Kapiloff MS, et al. The protein kinase A anchoring protein mAKAP coordinates two integrated cAMP effector pathways. Nature. 2005;437(7058):574-8.
29. Laurent AC, Breckler M, Berthouze M, Lezoualc'h F. Role of Epac in brain and heart. Biochemical Society transactions. 2012;40(1):51-7.
30. Seino S, Shibasaki T. PKA-dependent and PKA-independent pathways for cAMP-regulated exocytosis. Physiological reviews. 2005;85(4):1303-42.
31. Murray AJ, Shewan DA. Epac mediates cyclic AMP-dependent axon growth, guidance and regeneration. Molecular and cellular neurosciences. 2008;38(4):578-88.
32. Zhao K, Wen R, Wang X, Pei L, Yang Y, Shang Y, et al. EPAC inhibition of SUR1 receptor increases glutamate release and seizure vulnerability. The Journal of neuroscience : the official journal of the Society for Neuroscience. 2013;33(20):8861-5.
33. Gong B, Shelite T, Mei FC, Ha T, Hu Y, Xu G, et al. Exchange protein directly activated by cAMP plays a critical role in bacterial invasion during fatal rickettsioses. Proceedings of the National Academy of Sciences of the United States of America. 2013;110(48):19615-20.
34. Yan J, Mei FC, Cheng H, Lao DH, Hu Y, Wei J, et al. Enhanced leptin sensitivity, reduced adiposity, and improved glucose homeostasis in mice lacking exchange protein directly activated by cyclic AMP isoform 1. Molecular and cellular biology. 2013;33(5):918-26.

35. The kidney and the nephron. Available from: http://kvhs.nbed.nb.ca/gallant/biology/nephron_structure.html.
36. Guyton HH, J. E. Textbook of Medican Biology: Saunders, Elsevies; 2011.
37. Haraldsson B, Nystrom J, Deen WM. Properties of the glomerular barrier and mechanisms of proteinuria. Physiological reviews. 2008;88(2):451-87.
38. Komlosi P, Fintha A, Bell PD. Current mechanisms of macula densa cell signalling. Acta physiologica Scandinavica. 2004;181(4):463-9.
39. Wright FS, Schnermann J. Interference with feedback control of glomerular filtration rate by furosemide, triflocin, and cyanide. The Journal of clinical investigation. 1974;53(6):1695-708.
40. Ross MH, Pawline, W. Histology. A text and atlas. Wolters Kluwer, Lippincott Williams & Wilkins2011.
41. Sands JM, Layton HE. Advances in understanding the urine-concentrating mechanism. Annual review of physiology. 2014;76:387-409.
42. Oliver G, Schafer EA. The Physiological Effects of Extracts of the Suprarenal Capsules. The Journal of physiology. 1895;18(3):230-76.
43. Pickford M. The inhibition of water diuresis by pituitary (posterior lobe) extract and its relation to the water load of the body. The Journal of physiology. 1936;87(3):291-7.
44. Verney EB. The antidiuretic hormone and the factors which determine its release. Proceedings of the Royal Society of London Series B, Containing papers of a Biological character Royal Society. 1947;135(878):25-106.
45. Bankir L. Antidiuretic action of vasopressin: quantitative aspects and interaction between V1a and V2 receptor-mediated effects. Cardiovascular research. 2001;51(3):372-90.
46. Lolait SJ, O'Carroll AM, McBride OW, Konig M, Morel A, Brownstein MJ. Cloning and characterization of a vasopressin V2 receptor and possible link to nephrogenic diabetes insipidus. Nature. 1992;357(6376):336-9.
47. Chabardes D, Gagnan-Brunette M, Imbert-Teboul M, Gontcharevskaia O, Montegut M, Clique A, et al. Adenylate cyclase responsiveness to hormones in various portions of the human nephron. The Journal of clinical investigation. 1980;65(2):439-48.
48. Richardson DW, Robinson AG. Desmopressin. Annals of internal medicine. 1985;103(2):228-39.
49. Fushimi K, Uchida S, Hara Y, Hirata Y, Marumo F, Sasaki S. Cloning and expression of apical membrane water channel of rat kidney collecting tubule. Nature. 1993;361(6412):549-52.
50. Bagnasco SM, Peng T, Janech MG, Karakashian A, Sands JM. Cloning and characterization of the human urea transporter UT-A1 and mapping of the human Slc14a2 gene. American journal of physiology Renal physiology. 2001;281(3):F400-6.
51. Nielsen S, DiGiovanni SR, Christensen EI, Knepper MA, Harris HW. Cellular and subcellular immunolocalization of vasopressin-regulated water channel in rat kidney. Proceedings of the National Academy of Sciences of the United States of America. 1993;90(24):11663-7.
52. Kishore BK, Mandon B, Oza NB, DiGiovanni SR, Coleman RA, Ostrowski NL, et al. Rat renal arcade segment expresses vasopressin-regulated water channel and vasopressin V2 receptor. The Journal of clinical investigation. 1996;97(12):2763-71.
53. Nielsen S, Chou CL, Marples D, Christensen EI, Kishore BK, Knepper MA. Vasopressin increases water permeability of kidney collecting duct by inducing translocation of aquaporin-CD water channels to plasma membrane. Proceedings of the National Academy of Sciences of the United States of America. 1995;92(4):1013-7.

54. Katsura T, Gustafson CE, Ausiello DA, Brown D. Protein kinase A phosphorylation is involved in regulated exocytosis of aquaporin-2 in transfected LLC-PK1 cells. The American journal of physiology. 1997;272(6 Pt 2):F817-22.
55. Moeller HB, MacAulay N, Knepper MA, Fenton RA. Role of multiple phosphorylation sites in the COOH-terminal tail of aquaporin-2 for water transport: evidence against channel gating. American journal of physiology Renal physiology. 2009;296(3):F649-57.
56. Chou CL, Yip KP, Michea L, Kador K, Ferraris JD, Wade JB, et al. Regulation of aquaporin-2 trafficking by vasopressin in the renal collecting duct. Roles of ryanodine-sensitive Ca2+ stores and calmodulin. The Journal of biological chemistry. 2000;275(47):36839-46.
57. Wall SM, Han JS, Chou CL, Knepper MA. Kinetics of urea and water permeability activation by vasopressin in rat terminal IMCD. The American journal of physiology. 1992;262(6 Pt 2):F989-98.
58. Terris J, Ecelbarger CA, Nielsen S, Knepper MA. Long-term regulation of four renal aquaporins in rats. The American journal of physiology. 1996;271(2 Pt 2):F414-22.
59. Zhang C, Sands JM, Klein JD. Vasopressin rapidly increases phosphorylation of UT-A1 urea transporter in rat IMCDs through PKA. American journal of physiology Renal physiology. 2002;282(1):F85-90.
60. You G, Smith CP, Kanai Y, Lee WS, Stelzner M, Hediger MA. Cloning and characterization of the vasopressin-regulated urea transporter. Nature. 1993;365(6449):844-7.
61. Karakashian A, Timmer RT, Klein JD, Gunn RB, Sands JM, Bagnasco SM. Cloning and characterization of two new isoforms of the rat kidney urea transporter: UT-A3 and UT-A4. Journal of the American Society of Nephrology : JASN. 1999;10(2):230-7.
62. Hwang S, Gunaratne R, Rinschen MM, Yu MJ, Pisitkun T, Hoffert JD, et al. Vasopressin increases phosphorylation of Ser84 and Ser486 in Slc14a2 collecting duct urea transporters. American journal of physiology Renal physiology. 2010;299(3):F559-67.
63. Shayakul C, Smith CP, Mackenzie HS, Lee WS, Brown D, Hediger MA. Long-term regulation of urea transporter expression by vasopressin in Brattleboro rats. American journal of physiology Renal physiology. 2000;278(4):F620-7.
64. Cai Q, Nelson SK, McReynolds MR, Diamond-Stanic MK, Elliott D, Brooks HL. Vasopressin increases expression of UT-A1, UT-A3, and ER chaperone GRP78 in the renal medulla of mice with a urinary concentrating defect. American journal of physiology Renal physiology. 2010;299(4):F712-9.
65. Laroche-Joubert N, Marsy S, Michelet S, Imbert-Teboul M, Doucet A. Protein kinase A-independent activation of ERK and H,K-ATPase by cAMP in native kidney cells: role of Epac I. The Journal of biological chemistry. 2002;277(21):18598-604.
66. Li Y, Konings IB, Zhao J, Price LS, de Heer E, Deen PM. Renal expression of exchange protein directly activated by cAMP (Epac) 1 and 2. American journal of physiology Renal physiology. 2008;295(2):F525-33.
67. Kopperud R, Rygh, C., Karlsen, T., Krakstad, C., Hoivik, E., Tenstad, O., Selheim, F., Lidén, Å., Madsen, L., Pavlin, T., Taxt, T., Curry, F., Kristiansen, K., Reed, R., Døskeland, S. O. Increased microvascular permeability in mice lacking Epac1. In press.
68. Honegger KJ, Capuano P, Winter C, Bacic D, Stange G, Wagner CA, et al. Regulation of sodium-proton exchanger isoform 3 (NHE3) by PKA and exchange protein directly activated by cAMP (EPAC). Proceedings of the National Academy of Sciences of the United States of America. 2006;103(3):803-8.
69. Carraro-Lacroix LR, Malnic G, Girardi AC. Regulation of Na+/H+ exchanger NHE3 by glucagon-like peptide 1 receptor agonist exendin-4 in renal proximal tubule cells. American journal of physiology Renal physiology. 2009;297(6):F1647-55.

70. Yip KP. Epac-mediated Ca(2+) mobilization and exocytosis in inner medullary collecting duct. American journal of physiology Renal physiology. 2006;291(4):F882-90.
71. Umenishi F, Narikiyo T, Vandewalle A, Schrier RW. cAMP regulates vasopressin-induced AQP2 expression via protein kinase A-independent pathway. Biochimica et biophysica acta. 2006;1758(8):1100-5.
72. Kortenoeven ML, Trimpert C, van den Brand M, Li Y, Wetzels JF, Deen PM. In mpkCCD cells, long-term regulation of aquaporin-2 by vasopressin occurs independent of protein kinase A and CREB but may involve Epac. American journal of physiology Renal physiology. 2012;302(11):F1395-401.
73. Wang Y, Klein JD, Blount MA, Martin CF, Kent KJ, Pech V, et al. Epac regulates UT-A1 to increase urea transport in inner medullary collecting ducts. Journal of the American Society of Nephrology : JASN. 2009;20(9):2018-24.
74. Frohlich O, Klein JD, Smith PM, Sands JM, Gunn RB. Regulation of UT-A1-mediated transepithelial urea flux in MDCK cells. American journal of physiology Cell physiology. 2006;291(4):C600-6.
75. Yano N, Suzuki D, Endoh M, Zhao TC, Padbury JF, Tseng YT. A novel phosphoinositide 3-kinase-dependent pathway for angiotensin II/AT-1 receptor-mediated induction of collagen synthesis in MES-13 mesangial cells. The Journal of biological chemistry. 2007;282(26):18819-30.
76. Jackson EK, Raghvendra DK. The extracellular cyclic AMP-adenosine pathway in renal physiology. Annual review of physiology. 2004;66:571-99.
77. Lee YJ, Kim MO, Ryu JM, Han HJ. Regulation of SGLT expression and localization through Epac/PKA-dependent caveolin-1 and F-actin activation in renal proximal tubule cells. Biochimica et biophysica acta. 2012;1823(4):971-82.
78. Weinman EJ, Minkoff C, Shenolikar S. Signal complex regulation of renal transport proteins: NHERF and regulation of NHE3 by PKA. American journal of physiology Renal physiology. 2000;279(3):F393-9.
79. Kone BC. Renal H,K-ATPase: structure, function and regulation. Mineral and electrolyte metabolism. 1996;22(5-6):349-65.
80. Haslene-Hox H, Oveland E, Berg KC, Kolmannskog O, Woie K, Salvesen HB, et al. A new method for isolation of interstitial fluid from human solid tumors applied to proteomic analysis of ovarian carcinoma tissue. PloS one. 2011;6(4):e19217.
81. Semaeva E, Tenstad O, Skavland J, Enger M, Iversen PO, Gjertsen BT, et al. Access to the spleen microenvironment through lymph shows local cytokine production, increased cell flux, and altered signaling of immune cells during lipopolysaccharide-induced acute inflammation. J Immunol. 2010;184(8):4547-56.
82. Doskeland SO, Haga HJ. Measurement of adenosine 3':5'-cyclic monophosphate by competitive binding to salt-dissociated protein kinase. The Biochemical journal. 1978;174(2):363-72.
83. Jensen BO, Kleppe R, Kopperud R, Nygaard G, Doskeland SO, Holmsen H, et al. Dipyridamole synergizes with nitric oxide to prolong inhibition of thrombin-induced platelet shape change. Platelets. 2011;22(1):8-19.
84. Soodvilai S, Jia Z, Wang MH, Dong Z, Yang T. mPGES-1 deletion impairs diuretic response to acute water loading. American journal of physiology Renal physiology. 2009;296(5):F1129-35.
85. Ecelbarger CA, Kim GH, Wade JB, Knepper MA. Regulation of the abundance of renal sodium transporters and channels by vasopressin. Experimental neurology. 2001;171(2):227-34.

86. Helms MN, Chen XJ, Ramosevac S, Eaton DC, Jain L. Dopamine regulation of amiloride-sensitive sodium channels in lung cells. American journal of physiology Lung cellular and molecular physiology. 2006;290(4):L710-L22.
87. Rubera I, Loffing J, Palmer LG, Frindt G, Fowler-Jaeger N, Sauter D, et al. Collecting duct-specific gene inactivation of alphaENaC in the mouse kidney does not impair sodium and potassium balance. The Journal of clinical investigation. 2003;112(4):554-65.
88. Reif MC, Troutman SL, Schafer JA. Sodium transport by rat cortical collecting tubule. Effects of vasopressin and desoxycorticosterone. The Journal of clinical investigation. 1986;77(4):1291-8.
89. Field MJ, Stanton BA, Giebisch GH. Influence of ADH on renal potassium handling: a micropuncture and microperfusion study. Kidney international. 1984;25(3):502-11.
90. Perucca J, Bichet DG, Bardoux P, Bouby N, Bankir L. Sodium excretion in response to vasopressin and selective vasopressin receptor antagonists. Journal of the American Society of Nephrology : JASN. 2008;19(9):1721-31.
91. Chang YL, Lin AT, Chen KK. Short-term effects of desmopressin on water and electrolyte excretion in adults with nocturnal polyuria. The Journal of urology. 2007;177(6):2227-9; discussion 30.
92. Butcher RW, Sutherland EW. Adenosine 3',5'-phosphate in biological materials. I. Purification and properties of cyclic 3',5'-nucleotide phosphodiesterase and use of this enzyme to characterize adenosine 3',5'-phosphate in human urine. The Journal of biological chemistry. 1962;237:1244-50.
93. Ashman DF, Lipton R, Melicow MM, Price TD. Isolation of adenosine 3', 5'-monophosphate and guanosine 3', 5'-monophosphate from rat urine. Biochemical and biophysical research communications. 1963;11:330-4.
94. van Aubel RA, Smeets PH, Peters JG, Bindels RJ, Russel FG. The MRP4/ABCC4 gene encodes a novel apical organic anion transporter in human kidney proximal tubules: putative efflux pump for urinary cAMP and cGMP. Journal of the American Society of Nephrology : JASN. 2002;13(3):595-603.
95. Kaminsky NI, Broadus AE, Hardman JG, Jones DJ, Jr., Ball JH, Sutherland EW, et al. Effects of parathyroid hormone on plasma and urinary adenosine 3',5'-monophosphate in man. The Journal of clinical investigation. 1970;49(12):2387-95.
96. Butlen D, Jard S. Renal handling of 3'-5'-cyclic AMP in the rat. The possible role of luminal 3'-5'-cyclic AMP in the tubular reabsorption of phosphate. Pflugers Archiv : European journal of physiology. 1972;331(2):172-90.
97. Chase LR, Aurbach GD. Parathyroid function and the renal excretion of 3'5'-adenylic acid. Proceedings of the National Academy of Sciences of the United States of America. 1967;58(2):518-25.
98. Rieg T, Bundey RA, Chen Y, Deschenes G, Junger W, Insel PA, et al. Mice lacking P2Y2 receptors have salt-resistant hypertension and facilitated renal Na+ and water reabsorption. FASEB journal : official publication of the Federation of American Societies for Experimental Biology. 2007;21(13):3717-26.
99. Fenton RA, Chou CL, Stewart GS, Smith CP, Knepper MA. Urinary concentrating defect in mice with selective deletion of phloretin-sensitive urea transporters in the renal collecting duct. Proceedings of the National Academy of Sciences of the United States of America. 2004;101(19):7469-74.
100. Rojek A, Fuchtbauer EM, Kwon TH, Frokiaer J, Nielsen S. Severe urinary concentrating defect in renal collecting duct-selective AQP2 conditional-knockout mice. Proceedings of the National Academy of Sciences of the United States of America. 2006;103(15):6037-42.

101. Bagnasco SM, Peng T, Nakayama Y, Sands JM. Differential expression of individual UT-A urea transporter isoforms in rat kidney. Journal of the American Society of Nephrology : JASN. 2000;11(11):1980-6.
102. Dunn SR, Qi Z, Bottinger EP, Breyer MD, Sharma K. Utility of endogenous creatinine clearance as a measure of renal function in mice. Kidney international. 2004;65(5):1959-67.
103. Eisner C, Faulhaber-Walter R, Wang Y, Leelahavanichkul A, Yuen PS, Mizel D, et al. Major contribution of tubular secretion to creatinine clearance in mice. Kidney international. 2010;77(6):519-26.
104. Meyer MH, Meyer RA, Jr., Gray RW, Irwin RL. Picric acid methods greatly overestimate serum creatinine in mice: more accurate results with high-performance liquid chromatography. Analytical biochemistry. 1985;144(1):285-90.
105. Cullere X, Shaw SK, Andersson L, Hirahashi J, Luscinskas FW, Mayadas TN. Regulation of vascular endothelial barrier function by Epac, a cAMP-activated exchange factor for Rap GTPase. Blood. 2005;105(5):1950-5.
106. Fukuhara S, Sakurai A, Sano H, Yamagishi A, Somekawa S, Takakura N, et al. Cyclic AMP potentiates vascular endothelial cadherin-mediated cell-cell contact to enhance endothelial barrier function through an Epac-Rap1 signaling pathway. Molecular and cellular biology. 2005;25(1):136-46.
107. Del Prete D, Gambaro G, Lupo A, Anglani F, Brezzi B, Magistroni R, et al. Precocious activation of genes of the renin-angiotensin system and the fibrogenic cascade in IgA glomerulonephritis. Kidney international. 2003;64(1):149-59.
108. Greger R. Ion transport mechanisms in thick ascending limb of Henle's loop of mammalian nephron. Physiological reviews. 1985;65(3):760-97.
109. Hropot M, Fowler N, Karlmark B, Giebisch G. Tubular action of diuretics: distal effects on electrolyte transport and acidification. Kidney international. 1985;28(3):477-89.
110. Morgan T, Tadokoro M, Martin D, Berliner RW. Effect of furosemide on Na+ and K+ transport studied by microperfusion of the rat nephron. The American journal of physiology. 1970;218(1):292-7.
111. Mutig K, Kahl T, Saritas T, Godes M, Persson P, Bates J, et al. Activation of the bumetanide-sensitive Na+,K+,2Cl- cotransporter (NKCC2) is facilitated by Tamm-Horsfall protein in a chloride-sensitive manner. The Journal of biological chemistry. 2011;286(34):30200-10.
112. Caceres PS, Ares GR, Ortiz PA. cAMP stimulates apical exocytosis of the renal Na(+)-K(+)-2Cl(-) cotransporter NKCC2 in the thick ascending limb: role of protein kinase A. The Journal of biological chemistry. 2009;284(37):24965-71.
113. Meade P, Hoover RS, Plata C, Vazquez N, Bobadilla NA, Gamba G, et al. cAMP-dependent activation of the renal-specific Na+-K+-2Cl- cotransporter is mediated by regulation of cotransporter trafficking. American journal of physiology Renal physiology. 2003;284(6):F1145-54.